DYNAMIC ANALYSIS OF NONLINEAR ROTOR-HOUSING SYSTEMS

prepared for

George C. Marshall

Space Flight Center

Alabama 35812

under

CONTRACT NAS8 - 36293

Principal Investigator

Sherif T. Noah

Mechanical Engineering Department

Texas A&M University

College Station, Texas 77843

October 1988

TABLE OF CONTENTS

		Page
ABSTRACT		i
NOMENCLATURE		ii
LIST OF FIGURES		vii
1.	INTRODUCTION	1
	1.1 Background	1
	1.2 Objectives and Outline of Study	3
2.	NONLINEAR ROTORDYNAMIC ANALYSIS OF LARGE SYSTEMS	5
	2.1 Transient Analysis Methods	5
	2.2 Periodic Solutions	6
3.	APPLICATION TO ROTOR-HOUSING SYSTEMS	8
	3.1 The Model	8
	3.2 Method for Transient Analysis	16
	3.2a Transition matrix for the rotor	16
	3.2b Duhamel integral for housing	18
	3.2c The coupling forces	21
	3.2d The computational procedure	21
	3.3 Method for Obtaining Periodic Responses	22
	3.3a The computational harmonic balance method	24
	3.3b Determination of multiple solutions: A global Newton's method	34
4.	NUMERICAL EXAMPLES AND DISCUSSION	35
	4.1 Transient Response	35
	4.2 Periodic Response	40
5.	CONCLUSIONS AND RECOMMENDATIONS	54
	5.1 Conclusions	54
	5.2 Recommendations	56
ACKNOWLEDGEMENT		57
REFERENCES		58

TABLE OF CONTENTS (Cont'd.)

Page

APPENDIX A

DISCRETIZED FORM OF TRANSITION MATRIX FORMULATION. . 62

APPENDIX B

DISCRETIZED FORM OF THE DUHAMEL INTEGRAL SOLUTION. . 67

APPENDIX C

FOURTH ORDER RUNGE-KUTTA WITH ITERATION. 78

ABSTRACT

Nonlinear analysis methods are developed which will enable the reliable prediction of the dynamic behavior of the space shuttle main engine (SSME) turbopumps in the presence of bearing clearances and other local nonlinearities.

A computationally efficient convolution method, based on discretized Duhamel and transition matrix integral formulations, is developed for the transient analysis. In the formulation, the coupling forces due to the nonlinearities are treated as external forces acting on the coupled subsystems. Iteration is utilized to determine their magnitudes at each time increment. The method is applied to a nonlinear generic model of the high pressure oxygen turbopump (HPOTP). As compared to the fourth order Runge Kutta numerical integration methods, the convolution approach proved to be more accurate and highly more efficient.

For determining the nonlinear, steady-state periodic responses, an incremental harmonic balance (IHB) method was also developed. The method was successfully used to determine dominantly harmonic and subharmonic (subsynchronous) responses of the HPOTP generic model with bearing clearances. A reduction method similar to the impedance formulation utilized with linear systems is used to reduce the housing-rotor models to their coordinates at the bearing clearances.

Recommendations are included for further development of the method, for extending the analysis to aperiodic and chaotic regimes and for conducting critical parametric studies of the nonlinear response of the current SSME turbopumps.

NOMENCLATURE

$\{A_m^0\}$ = Cosine coefficients associated with Master degrees of freedom

$\{\Delta A_m\}$ = Incremental vector of $\{A_m^0\}$

A_{nx}^i, A_{ny}^i = nth cosine coefficient of the steady state solution in x, y-direction at ith node

$\{A_s^0\}$ = Cosine coefficients associated with Slave degrees of freedom

B_{nx}^i, B_{ny}^i = nth since coefficient of the steady state solution in x, y-direction at ith node

$[\tilde{C}]$ = Structural damping matrix

$\{C_n\}$ = Constant cosine coefficient vector of nonlinear force

C_{nx}, C_{ny} = nth cosine coefficient of nonlinear force in x, y-direction

$\{C_m^0\}$ = Cosine coefficients of nonlinear force associated Master degree of freedom

$\{C_s^0\}$ = Cosine coefficients of nonlinear force associated Slave degree of freedom

[D] = Generalized damping matrix of rotor model

$\{D_n\}$ = Constant sine coefficient vector of nonlinear force

D_{nx}, D_{ny} = nth sine coefficient of nonlinear force in x, y-direction

e = Mass eccentricity of disks

$\{f_{ix}, f_{iy}\}$ = Nonlinear restoring force vector in x, y-direction at ith node

$\{F_E\}$ = Imbalance forces on rotor

$\{F\}$ = The coupling force vector on the housing due to the rotor

$\{g_c, g_s\}$ = Imbalance force vector of cosine, sine terms

$[G]$ = Gyroscopic matrix

H_{ix}, H_{iy} = x,y rectilinear housing displacement at ith node

$[I]$ = Identity matrix

$[K]$ = Structural stiffness matrix

K_b = Bearing stiffness

$[\bar{K}]$ = Equivalent constant coefficient stiffness matrix

$[M]$ = Mass matrix

$\{P\}$ = Generalized force (modal force)

$\{q\}$ = Generalized displacement (modal displacement)

$[Q]$ = Transition matrix

$\{\varrho_m\}$ = Trigonometric coefficients associated with Master degrees of freedom

$\{\varrho^0_{mn}\}$ = Trigonometric coefficients with nth harmonic mode in Master degree of freedom

$\{\Delta\varrho^0_{mn}\}$ = Incremental vector form of $\{\varrho^0_{mn}\}$

$\{\varrho_s\}$ = Trigonometric coefficients associated Slave degrees of freedom

$\{\Delta r\}$ = Overall incremental coefficient vector

R_{ix}, R_{iy} = x,y rectilinear displacement at ith node

$[S]$ = Total trigonometric coefficient matrix

$[\bar{S}]$ = Equivalent trigonometric coefficient matrix

$[\overline{S_n}]$ = Overall coefficient matrix

t = Time

T = Time increment

t_i = Time at iT

$\{u\}$ = $\begin{Bmatrix} q \\ \dot{q} \end{Bmatrix}$, Generalized coordinates of rotor

$\{\bar{U}\}$ = equivalent trigonometric force vector

$\{\Delta v\}$ = Overall incremental coefficient vector of nonlinear force

$\{W\}$ = Constant trigonometric coefficient vector of nonlinear force

$\{W_m\}$ = Trigonometric coefficients of nonlinear force associated with Master degree of freedom

$\{W^0_{mn}\}$ = Trigonometric vector of nonlinear force with nth harmonic mode in Master degree of freedom

$\{\Delta W_{mn}\}$ = Incremental vector of $\{W^0_{mn}\}$

$\{z\}$ = Overall force vector

β_{iz}, β_{iy} = Rational displacement in x,y-direction at ith node

δ = Gap size

ν = Subharmonic ratio

$[\alpha]$ = The rotor state matrix

$[\Lambda]$ = Diagonal eigenvalue matrix

$\dot{\phi} = \omega$ = Spinning speed of rotor

$[\Psi]$ = Normalized modal matrix

ξ = Damping ratio

ω_n, ω_d = Natural frequency and damped natural frequency

$[0]$ = Null matrix

Superscript

i = ith node

Y = The node number at which disk is located

Subscript

B, b = Bearing related term

H = Housing related term

E = External, imbalance

I = Coupling

i = ith time increment

L = Total number of degrees of freedom associated with linear motion

N = Total number of degrees of freedom associated with nonlinear coupling nodes

M = Total number of degrees of freedom (M = L+N)

R = Rotor related term

m = Master degree of freedom

n = nth harmonic mode

s = Slave degree of freedom

x = x-direction

y = y-direction

x,y,z = x,y,z-direction

Other Symbols

{ } = Vector

[ ] = Square matrix

[` .] = Diagonal matrix

{ } = Column matrix

$[\ ]^{-1}$ = Inverse of a matrix

$[\ ]^{T}$ = Transpose of a matrix

LIST OF FIGURES

		Page
Figure 1	Complex rotor system with flexible housing . .	9
Figure 2	The rotor coordinate system.	10
Figure 3	Rotor and housing displacements at bearing location	13
Figure 4	Nonlinear bearing force, F_G, due to K_G	14
Figure 5	The generic model.	36
Figure 6	Running speed of rotor	38
Figure 7	CPU plot of Hybrid method and Runge Kutta method	38
Figure 8a	Force in linear bearing 1 (δ = 0).	39
Figure 8b	Force in nonlinear bearing ($\delta = 5 \times 10^{-4}$ in) .	39
Figure 9	Force in nonlinear bearing 1 during shutdown .	41
Figure 10a	Relative displacement of rotor in Y-direction at linear bearing 1	42
Figure 10b	Relative displacement of rotor in Y-direction at nonlinear bearing 1	42
Figure 11	Critical speed of linear generic model at bearing 1; eccentricity = 0.5 mils, no damping, no gyroscopic effects	43
Figure 12	Critical speed map for the linear generic model; no damping.	44
Figure 13	Trajectory for subharmonic motion of order 1/2; gap = 0.5 mils, eccentricity = 0.5 mils, side force = 10 lbs, speed = 4210 rad/sec. . .	46
Figure 14	Trajectory for subharmonic motion of order 1/2; gap = 0.2 mils, eccentricity = 0.5 mils, side force = 10 lbs, speed = 4210 rad/sec. . .	47

LIST OF FIGURES (Cont'd.)

Page

Figure 15 Trajectory for subharmonic motion of order 1/2; gap = 0.7 mils, eccentricity = 0.5 mils, side force = 10 lbs, speed = 4210 rad/sec. . . 48

Figure 16 Trajectory for subharmonic motion of order 1/2; gap = 0.5 mils, eccentricity = 0.5 mils, side force = 100 lbs, speed = 4210 rad/sec. . . 49

Figure 17 Gap size effect on subharmonic motion of order 1/2; eccentricity = 0.5 mils, speed = 4210 rad/sec 51

Figure 18 Mass eccentricity effect on subharmonic motion of order 1/2; gap size = 0.5 mils, speed = 4210 rad/sec 52

1. INTRODUCTION

1.1 Background

Modern complex rotating machinery contain various sources of strong nonlinearities. These include clearances in bearings, gears and splines, rubbing in splines, seals and rotor blades, squeeze film dampers and other fluid effects. Observed nonlinear behavior of actual rotor systems includes jump discontinuities (Erich, 1966), large subsynchronous motion (Bently, 1979, Muszynska, 1984, and Beatty, 1985), quasi-periodic response and possible chaos (Neilson and Barr, 1988). As stated by Nataraj and Nelson (1987), the future developments in modern machines heavily depends on the ability to identify, understand, mathematically model and analyze systems involving nonlinear components.

The turbopumps of the space shuttle main engine (SSME) are complex rotor-housing systems. Their response and stability can be critically dependent on the coupling forces between their flexible rotors and housings, transmitted through the working fluids, seals and bearings. Of particular concern is the effect of the existing essential deadband clearances between the ball bearings and housing. These clearances cause a turbopump rotor to respond as a nonlinear dynamic system. In general, the rotor-housing system could, consequently, exhibit undesirable subharmonic, combination and internal resonances

(Tondl, 1965). It could also respond in an aperiodic or unpredictable chaotic fashion (Shaw and Holmes, 1983 and Neilson and Barr, 1988). The transient response of the rotor in passing through a critical speed can be quite different in the presence of a nonlinearity (Ishida et. al., 1987).

Childs and Moyer (1984), using a Runge-Kutta integration scheme, carried out a transient nonlinear analysis of the HPOTP (high pressure oxygen turbopump) of the SSME and reproduced a subsynchronous rotor response similar to that observed in experimental test results. They attributed the subsynchronous response to the presence of the bearing clearances and destabilizing impeller-diffuser forces. Glease and Bukley (1984) examined the effects of bearing deadbands on a modified Jeffcott model subjected to seal cross coupling forces and described responses of the rotor to imbalance forces of the subsynchronous, synchronous and nonperiodic type. Using a similar model as that of Glease (1984), Day (1987) and Zalik (1987) addressed some aspects of the response in the presence of bearing clearances and cross coupled seal forces as leading to a limit cycle with a "nonlinear natural frequency." For certain ranges of the systems parameters, quasi-periodic response of the rotor can occur.

Quite often, it is essential to determine the steady state periodic response of rotor systems in the form of self excited limit cycles or forced motion due to rotating unbalance. Accurate prediction of the nonlinear periodic responses and

their stability plays a central role in developing a complete picture of the dynamic behavior of nonlinear rotor systems as a function of their parameters. Efficient general methods are obviously needed for determining directly possible periodic solutions of large rotor-housing systems involving nonlinearities. In contrast, a direct numerical integration method used to obtain the steady state periodic solutions:

a. Will require much longer computational time for the relatively lightly damped rotor systems to settle to a steady state.

b. Will determine only stable periodic responses and not the unstable solutions which may be used to indicate the onsets of transition to chaotic responses.

c. Might miss a close-by large steady state solution from among multiple nonlinear solutions due to an unfortunate selection of initial conditions.

1.2 Objectives and Outline of Study

The main objective of this study is to develop reliable and efficient analytical-computational methods of the nonlinear dynamic analysis of large, rotor-housing systems such as the turbopumps of the space shuttle main engines (SSME).

The present study examines some aspects of the nonlinear behavior of a general multi-disk rotor-housing system. For that purpose, a generic model of the SSME turbopumps proposed

by Davis et al. (1984) is used to which new nonlinear analysis methods developed by the present author and co-researchers are applied. One of the methods extends an incremental harmonic balance method developed earlier by Choi and Noah (1987) to the determination of the periodic response of multi-degree of freedom rotor systems. Associated with this method, a Quasi-Newton method was also developed to enable the determination of possible multiple solutions for a given set of rotor parameters. For the transient analysis, a convolution method is fully developed which takes advantage of the fact that a turbo-pump system consists of a linear rotor model coupled to a linear housing model through a local nonlinearity, that is, bearings with clearances, to construct a highly efficient and accurate computational procedure. The method can be equally applied in presence of other coupling nonlinearities between the rotor and housing.

2. NONLINEAR ROTORDYNAMIC ANALYSIS OF LARGE SYSTEMS

2.1 Transient Analysis Methods

The direct numerical integration for determining the transient response of larger nonlinear rotor-flexible housing systems may require excessive computational time and involve unacceptable round-off errors. To remedy these problems different procedures have been developed by analysts to determine the transient response of large order rotor systems. The procedures can be recognized as falling under one of two basic approaches. Those using physical or modal coordinates of the complete system and those using the coordinates of the individual components of the system. The methods also differ in the numerical integration methods selected for the analysis. A comprehensive review of existing transient analysis techniques can be found in a report by Noah (1986).

An effective method which proves to be highly efficient in determining the transient response of linear systems under specified general excitations is by utilizing the Duhamel integral, or more generally, the transition matrix of the system (Meirovitch, 1980). Von Pragenau (1981) utilized the transition matrix with a linear system, stating that it offers the simplicity of the Euler method without requiring small steps. Von Pragenau maintained that for systems with constant coefficients, the stability and accuracy of the method are

acquired through the closed form solution of the transition matrix.

In the present study, the convolution methods (Duhamel and transition) are shown to be very effective when extended for application to linear systems with local nonlinearities. The forces at the nonlinear locations are treated as the external forces on the systems or subsystems and iteration is used at each time increment to determine the magnitude of the forces for subsequent increments.

The convolution approach is applied to a general rotor-housing system with rotor imbalance during start-up or shut-down. In the present work, eigen-coordinates are used to represent both housing and rotor. The local nonlinearities were taken as deadband clearances at the rolling element bearings which support the rotor in its housing as in the SSME turbopumps. The integral formulation of the rotor motion is represented by its transition matrix and that of the housing by a Duhamel integral. Kubomura (1985) used a Duhamel integration method to achieve dynamic condensation of a substructure to its coupling points to other structures. Convolution was also used by Tongue and Dowell (1983), and Clough and Wilson (1979) to reduce system coordinates to that of the nonlinearities.

2.2 Periodic Solutions

Several methods have recently been advanced for determining the periodic response of low order nonlinear rotor

systems (Yamamoto 1954, Childs 1982, Saito 1985, and Choi and Noah 1987). For application to larger, multi-disk rotor systems, Nataraj and Nelson (1987) developed a periodic solution method based on a collocation approach for the response of the rotor. They utilized a subsystem approach (Cipra and Uicker, 1981) to reduce the size of the resulting system of algebraic equations.

In this report, a general approach for the determination of the synchronous and subsynchronous response of complex rotor systems is presented. The present work extends the harmonic balance method developed earlier (Saito 1985, and Choi and Noah 1987 and 1988) for a modified Jeffcott rotor model with bearing clearances to the determination of the periodic response of nonlinear multi-disk rotor systems with flexible housings.

It is shown that the harmonic balance method, as applied to a large, rotor-housing system with bearing clearances, can be made to be highly efficient. This is achieved by using a version of an impedance formulation in which the system is reduced to its displacements at the bearing clearances. (See Noah, 1984 and Fan and Noah, 1989). In this case, the impedance method is applied to each of the harmonic components of the assumed periodic solution.

3. APPLICATION TO ROTOR-HOUSING SYSTEMS

3.1 The Model

A representative complex rotor system with flexible housing is shown in Fig. 1. The particular model shown in which the present method can be readily applied, represents the high pressure oxygen turbopump (HPOTP) of the space shuttle main engine (SSME). The interaction forces between rotor and housing include various seal, impeller, turbine tip clearance, bearing clearance and fluid side forces.

a. - Rotor

The equation of small transverse motion, $\{R\}$ of the rotor under transient external and imbalance forces may be written as

$$[M]_R \{\ddot{R}\} - \dot{\phi} [G] \{\dot{R}\} + [K]_R \{R\} = \{F_I\}_R + \{F_E\}_R \quad (1)$$

In equation (1), $\{R\}$ represents the translational and rotational displacements and only includes those displacements which are associated with masses and diametral moments of inertia. Other displacements are reduced out using static condensation. The spinning speed of the rotor is denoted by $\dot{\phi}$ (see Fig. 2), [G] is the gyroscopic matrix corresponding to the attached disks, $\{F_I\}_R$ represents the coupling forces on the rotor due to coupling to the housing while $\{F_E\}_R$ represents the external forces including the imbalance forces.

$$\text{Let } \{R\} = [\Psi]_R \{q\}_R \quad (2)$$

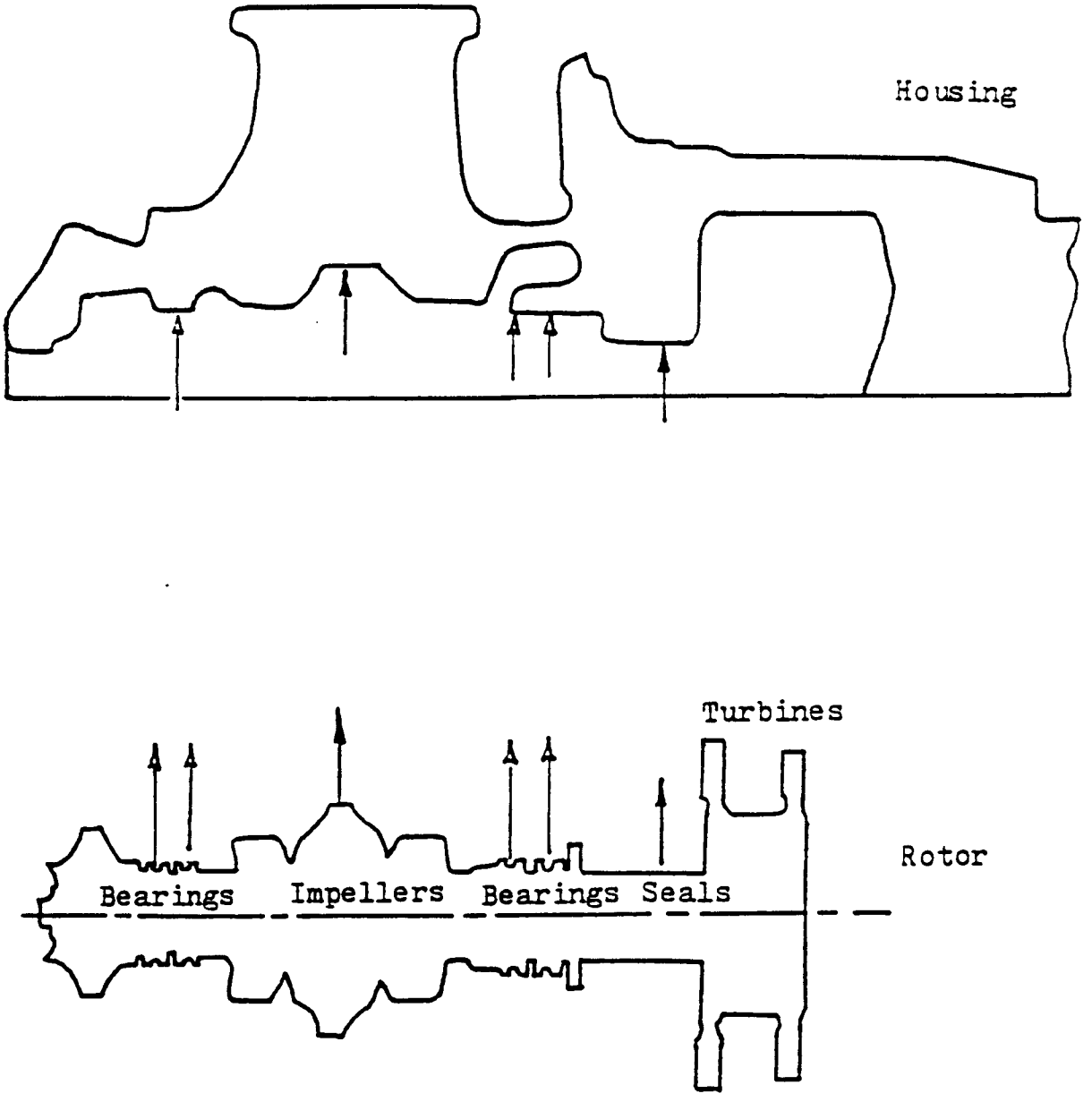

Figure 1. Complex rotor system with flexible housing.

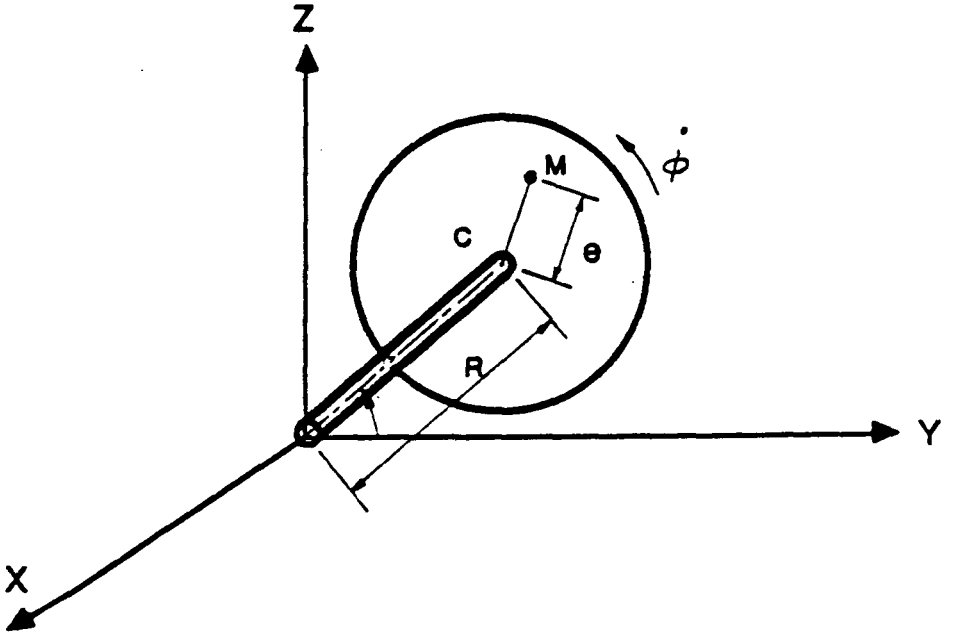

Figure 2. The rotor coordinate system.

in which $[\Psi]_R$ is the modal matrix, normalized with respect to the mass matrix of the nonspinning rotor and $\{q\}_R$ is the associated modal coordinates.

Using the modal transformation (2), equation (1) is written in the form

$$\{\ddot{q}\}_R - [\Psi]_R^T \dot{\phi} [G]_R [\Psi]_R \{\dot{q}\}_R + [\hat{\Lambda}]_R \{q\}_R = [\Psi]_R^T (\{F_I\}_R + \{F_E\}_R) \tag{3}$$

Where $[\hat{\Lambda}]_R = [\hat{\omega}_n^2]_R$

ω_n are the natural frequencies of the nonspinning of the rotor. Adding a modal damping matrix $[\hat{C}]$ to equation (3) yields

$$\{\ddot{q}\}_R + [D]_R \{\dot{q}\}_R + [\hat{\Lambda}]_R \{q\}_R = [\Psi]_R^T (\{F_I\}_R + \{F_E\}_R) \tag{4}$$

where $$[D]_R = [\hat{C}]_R - [\Psi]_R^T \dot{\phi} [G]_R [\Psi]_R \tag{5}$$

$$[\hat{C}]_R = [\hat{2\xi\omega_n}]_R \tag{6}$$

b. Housing

The equation of motion of the housing may be expressed as

$$[M]_H \{\ddot{H}\} + [K]_H \{H\} = \{F_I\}_H \tag{7}$$

where $\{H\}$ represents the transverse and rotational displacements at each node in the Y and Z directions. In terms of the modal coordinates of the housing while uncoupled to the rotor, equation (7) takes the form (after adding a modal damping matrix)

$$\{\ddot{q}\}_H + [D]_H \{\dot{q}\}_H + [\Lambda]_H \{q\}_H = [\Psi]_H^T (\{F_I\}_H + \{F_E\}_H) \quad (8)$$

Where $$[D]_H = [C]_H = [2\xi\omega_n]_H \quad (9)$$

$$[\Lambda]_H = [\omega_n^2]_H \quad (10)$$

c. Coupling Forces

Forces due to linear coupling between rotor and housing may include the direct and cross coupling forces due to seal, impeller and turbine forces. The nonlinear coupling forces are taken as those due to the clearances between the rolling element bearings outer races and the housing. Fig. 3 shows a model for the gap at each of the loosely supported bearing.

The bearing force acting on the housing due to the stiffness, shown in Fig. 4 in the Y-direction, is

$$(F_B)_Y = K_{BY} (R - \delta) \frac{R_Y - H_Y}{R} \qquad \text{for } R \geq \delta$$

$$(F_B)_Y = 0 \qquad \text{for } R \leq \delta$$

Analogous equations hold for the Z direction, in which K_{BY} is the stiffness at the bearing support and

$$R = \sqrt{(R_Y - H_Y)^2 + (R_Z - H_Z)^2}$$

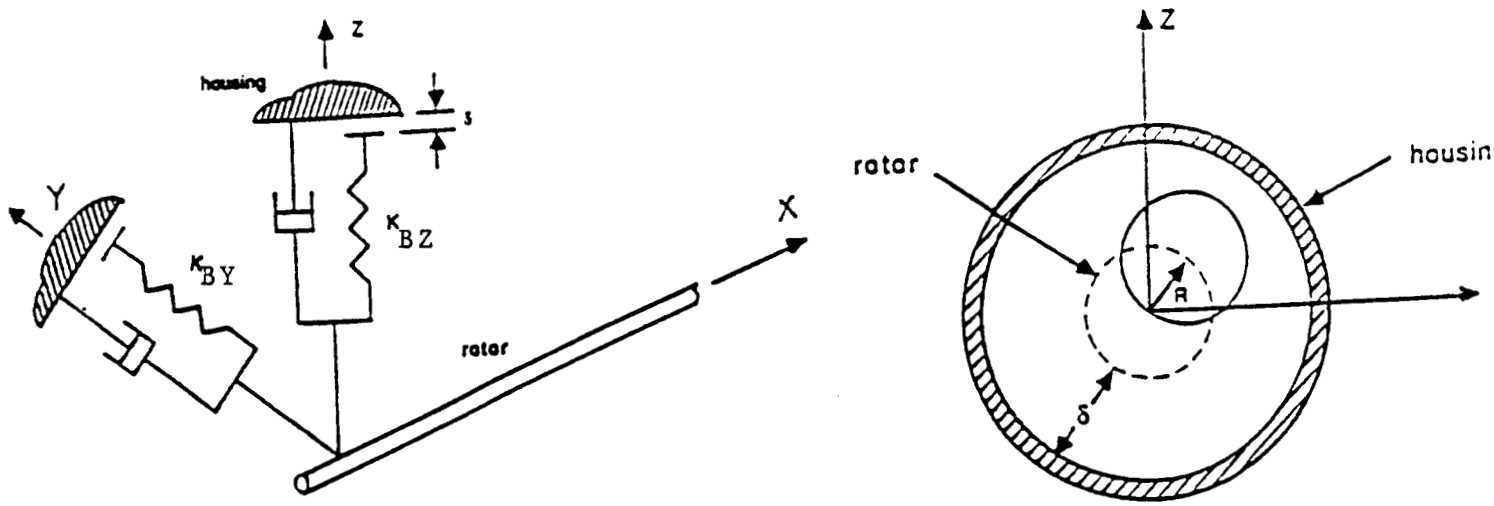

Figure 3. Rotor and housing displacements at bearing location.

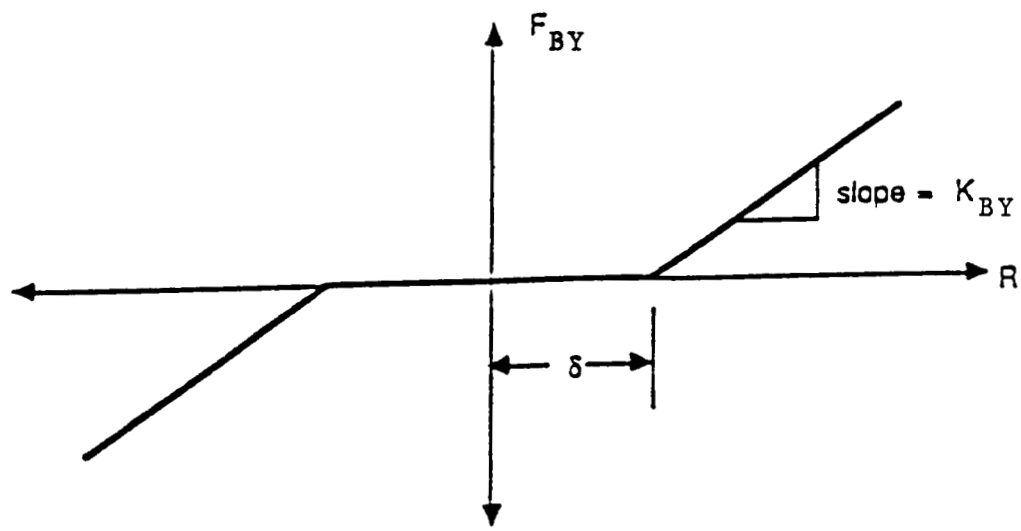

Figure 4. Nonlinear bearing force, in Y-direction F_{BY}, due to K_{BY}

where R_Y is the physical displacement of rotor in Y direction at the bearing location.

H_Y is the physical displacement of housing in Y direction at the bearing location.

R_Z is the physical displacement of rotor in Z direction at the bearing location.

H_Z is the physical displacement of housing in Z direction at the bearing location.

The bearing forces in the Y and Z-directions can be written as

$$(F_B)_Y = \overline{K}_{BY}(R_Y - H_Y) \tag{11}$$

$$(F_B)_Z = \overline{K}_{BZ}(R_Z - H_Z) \tag{12}$$

Where $$\overline{K}_B = K_B \left(1 - \frac{\delta}{R}\right) \text{ for } R \geq \delta \tag{13}$$

$$\overline{K}_B = 0 \qquad \text{for } R \leq \delta \tag{14}$$

3.2 Method for Transient Analysis

A hybrid method proposed by Noah et al. (1986) and (1988) is utilized here for the analysis of the coupled rotor-housing system. The displacements of the housing are best represented by a Duhamel integral. Due to the presence of the skew-symmetric gyroscopic terms, the equations of motion for the rotor are transformed to first order. The displacements of the rotor are expressed in terms of the transition matrix for the motion of the rotor.

3.2a Transition matrix for the rotor

The equations of motion of the rotor, equation (4), are cast in first order form,

$$\{\dot{u}\}_R = [\alpha]_R \{u\}_R + \{P\}_R \tag{15}$$

where $$[\alpha]_R = \begin{bmatrix} [0] & [I] \\ -[A]_R & -[D]_R \end{bmatrix} \tag{16}$$

$$\{P\}_R = \begin{Bmatrix} 0 \\ [\Psi]_R^T (\{F_I\}_R + \{F_E\}_R) \end{Bmatrix} \tag{17}$$

If the spinning speed is a function of time, the gyroscopic term of equation (5) is moved to the R.H.S. of equation (4). In this case, the coefficient matrices, given by equations (16) and (17), are replaced by

$$[\alpha]_R = \begin{bmatrix} [0] & [\hat{I}] \\ -[\hat{\Lambda}]_R & -[\hat{C}]_R \end{bmatrix} \tag{16'}$$

and

$$\{P\}_R = \begin{Bmatrix} 0 \\ [\Psi]_R^T (\{F_I\}_R + \{F_E\}_R) \end{Bmatrix} + \begin{Bmatrix} 0 \\ [\Psi]_R^T \dot{\phi}[G]_R[\Psi]_R\{\dot{q}\}_R \end{Bmatrix} \tag{17'}$$

In that case it may be computationally more efficient to use the Duhamel integral, rather than the transition matrix formulations to represent the rotor. The formulation using the Duhamel integral is applied to the housing as is shown later. In general, however, if the physical rather than the modal coordinates are used to describe the motion of the rotor, or if $\dot{\phi}$ is constant and is kept at the left hand side of the equations of motion, the transition matrix and not the Duhamel formulation method must be used.

The solution of equation (15) can be written as

$$\{u(t)\}_R = e^{[\alpha]_R t}\{u_o\} + \int_o^t e^{[\alpha]_R(t-\tau)}\{P(\tau)\}_R \, d\tau \tag{18}$$

where $$e^{[\alpha]_R t} = \sum_{k=0}^{\infty} \frac{[\alpha]_R^k t^k}{k!} = \text{transition matrix} \tag{19}$$

and $\{u_o\}$ is the initial generalized coordinates

Equation (18) can be cast in discretized form in which the generalized forces, $\{P\}_R$, are taken as varying linearly between time t_i and t_{i+1} so that

$$\{P(t)\} = \{P(t_i)\} + \frac{t - t_i}{T} \left(\{P(t_{i+1})\} - \{P(t_i)\}\right),$$

$$t_i \leq t \leq t_{i+1}$$

and $t_{i+1} = t_i + T$

Where T is a small increment in time. The discretized form of equation (18) can then be shown to take the form

$$\{u(t_{i+1})\}_R = [Q(T)]\ \{u(t_i)\}_R + \left([Q(T) - [\text{-I-}]\right)\ [\alpha]_R^{-1}\left(\{P(t_i)\}_R + [\alpha]_R^{-1}\ \frac{\{P(t_{i+1})\}_R - \{P(t_i)\}_R}{T}\right) - [\alpha]_R^{-1}\left(\{P(t_{i+1})\}_R - \{P(t_i)\}_R\right) \tag{20}$$

where $[Q(T)] = e^{[\alpha]_R T}$ (21)

3.2b Duhamel integral for housing

The symmetric form of the equations of motion of the housing allows expressing the modal displacements of the housing by a Duhamel integral. The integral formulation has the advantage of providing a closed form expression as opposed to conventional numerical integration schemes. Also this representation allows dealing directly with diagonal matrices which results in higher computational speed and accuracy.

Based on equation (8), the housing generalized coordinates can be expressed as

$$\{q(t)\}_H = [e^{-\xi\omega_n t} \cos \omega_d t] \{q(0)\}_H$$

$$+ [\frac{1}{\omega_d} e^{-\xi\omega_n t} \sin \omega_d t] (\{\dot{q}(0)\}_H + \xi\omega_n\{q(0)\}_H)$$

$$+ \int_0^t [\frac{1}{\omega_d} e^{-\xi\omega_n(t-\tau)} \sin \omega_d (t-\tau)] \{P(\tau)\}_H \, d\tau \qquad (22)$$

where $\{q(0)\}$, $\{\dot{q}(0)\}$ are initial solutions, ω_n, ω_d are undamped and damped natural frequencies of housing, ξ is damping ratio of housing, $\{P(t)\}_H = [\Psi]_H^T(\{F_I\}_H + \{F_E\}_H)$ the generalized forces act on housing.

The expression (22) is next written in discretized form, with the generalized forces taken as before as varying linearly within each time step, or

$$\{q(t_{i+1})\}_H = [e^{-at_{i+1}} \cos bt_{i+1}] \{q(0)\}_H$$

$$+ [\frac{1}{b} e^{-at_{i+1}} \sin bt_{i+1}](\{\dot{q}(0)\}_H + a\{q(0)\}_H)$$

$$+ \{\frac{\sin bt_{i+1}}{b(a^2+b^2)} \cdot EA_{i+1} + \frac{\cos bt_{i+1}}{b(a^2+b^2)} \cdot EB_{i+1}\} \qquad (23)$$

$$\{\dot{q}(t_{i+1})\}_H = [-e^{-at_{i+1}}(a \cos bt_{i+1} + b \sin bt_{i+1})]\{q(0)\}_H$$

$$+ [e^{-at_{i+1}}(-\frac{a}{b} \sin bt_{i+1} + \cos bt_{i+1})](\{\dot{q}(0)\}_H + a\{q(0)\}_H)$$

$$+ \{\frac{-a \sin bt_{i+1} + b \cos bt_{i+1}}{b(a^2+b^2)} \cdot EA_{i+1}$$

$$+ \frac{a \cos bt_{i+1} + b \sin bt_{i+1}}{b(a^2+b^2)} \cdot EB_{i+1}\} \quad (24)$$

$$a = \xi\omega_n \quad (25)$$

$$b = \omega_d \quad (26)$$

$$EA_{i+1} = e^{-aT} \cdot EA_i + A_{i+1} \quad (27)$$

$$EB_{i+1} = e^{-aT} \cdot EB_i + B_{i+1} \quad (28)$$

$$EA_i = e^{-at_{i-1}} A_1 + e^{-at_{i-2}} A_2 + ... + A_i \quad (29)$$

$$EB_i = e^{-at_{i-1}} B_1 + e^{-at_{i-2}} B_2 + ... + B_i \quad (30)$$

$$A_{i+1} = P_{i+1} (a \cos bt_{i+1} + b \sin bt_{i+1})$$

$$- \frac{P_{i+1} - P_i}{T(a^2+b^2)} (a^2 \cos bt_{i+1} + 2ab \sin bt_{i+1} - b^2 \cos bt_{i+1})$$

$$+ \frac{P_{i+1} - P_i}{T(a^2+b^2)} e^{-aT} (a^2 \cos bt_i + 2ab \sin bt_i - b^2 \cos bt_i)$$

$$- P_i e^{-aT} (a \cos bt_i + b \sin bt_i) \quad (31)$$

$$B_{i+1} = P_{i+1} (a \sin bt_{i+1} - b \cos bt_{i+1})$$

$$- \frac{P_{i+1} - P_i}{T(a^2+b^2)} (a^2 \sin bt_{i+1} - 2ab \cos bt_{i+1} - b^2 \sin bt_{i+1})$$

$$+ \frac{P_{i+1} - P_i}{T(a^2+b^2)} e^{-aT} (a^2 \sin bt_i - 2ab \cos bt_i - b^2 \sin bt_i)$$

$$- P_i e^{-aT} (a \sin bt_i - b \cos bt_i) \qquad (32)$$

P is element of vector $\{P\}$.

3.2c The coupling forces

The coupling forces acting on the housing are given by

$$\{F_I\}_H = [K]_I (\{R\} - \{H\}) + [C]_I (\{\dot{R}\} - \{\dot{H}\}) \qquad (33)$$

and those on the rotor are

$$\{F_I\}_R = - \{F_I\}_H$$

Where $[K]_I$ and $[C]_I$ are the coupling stiffness and damping matrices, respectively. The coupling stiffness matrix includes the updated bilinear bearing stiffness at each iteration.

3.2d The computational procedure

For the responses at time $t = t_{i+1}$, the coupling forces between the housing and rotor are unknown. An iterative technique is used to calculate these forces. The following iterative loop is used in both the Hybrid and Runge Kutta methods:

If the responses at $t = t_i$ are known and responses at $t = t_{i+1}$ are desired then:

(a) Set $\{F_I(t_{i+1})\} = \{F_I(t_i)\}$

(b) Calculate $\{P\}_R$ and $\{P\}_H$

(c) Solve $\{u(t_{i+1})\}_R$ and $\{q(t_{i+1})\}_H$, $\{\dot{q}(t_{i+1})\}_H$ by the Hybrid method (or the Runge Kutta method). Calculate the Euclidean norm of $\{u(t_{i+1})\}_R$ and $\{q(t_{i+1})\}_H$.

(d) Transfer $\{u(t_{i+1})\}_R$ and $\{q(t_{i+1})\}_H$, $\{\dot{q}(t_{i+1})\}_H$ back to physical coordinates, then a new connection force $\{F_I(t_{i+1})\}$ can be calculated.

(e) If the Euclidean norms of two consecutive iterations of both rotor and housing are close enough then stop the iteration and go to step (f), otherwise go to (b).

(f) Move a time increment and go to (a) until t reaches a specified time for terminating the run.

3.3 Method for Obtaining Periodic Responses

A typical multi-disk rotor interacting with its flexible housing through rolling element bearings with deadband clearances is considered. The equations of motion of the rotor can be recast from equation (1) in matrix form as

$$[M]_R\{\ddot{R}\} + [C]_R\{\dot{R}\} + [K]_R\{R\} = \{F_C\}_R + \{F_I\}_R \qquad (34)$$

Where $[C]_R$ includes damping and gyroscopic terms. The displacement vector $\{R\}$ is defined as

$$\{R\} = \{R_{1x}, R_{1y}, \ldots, \beta_{My}, \beta_{Mx}\}$$

where R_i and β_i stand for displacement and rotation, respectively, and subscript M represents the total node number.

In particular, the forces in the y-direction on the bearings with clearances are expressed as

$$F_{bmy} = K_{bmy}(R_{my} - H_{ny})\left(1 - \frac{\delta}{\sqrt{(R_{my}-H_{ny})^2 + (R_{mz}-H_{nz})^2}}\right) \qquad (35)$$

where m and n denote the bearing node numbers on the rotor and housing, respectively, and y and z denote the y-axis and z-axis of the rotor and housing coordinates. The rotor displacements are denoted by R while H denotes the housing response. The symbol δ represents the size of the deadband clearance between a bearing and the housing.

The bearing forces, F_{bmy} or F_{bmz}, will vanish if δ is larger than the radial displacement of the rotor relative to the housing which is the denominator in equation (35), otherwise the bearing forces will be as given by equation (35). A similar expression can be written for the nonlinear bearing forces in the z-direction, which are denoted by F_{bmz}.

The equations of motion for the housing can be written in the matrix form as

$$[M]_H\{\ddot{H}\} + [C]_H\{\dot{H}\} + [K]_H\{H\} = \{F_I\}_H \qquad (36)$$

where $[C]_H$ represents proportional equivalent viscous damping coefficients.

In order to reduce the system to its displacements at the nonlinear bearing supports, the equations of motion need to be modified. This is achieved using a subsystem approach. The coordinate vector can be modified so that the transverse displacements at the gap are listed first

$$\{R\} = \{R_{1y,2y,\ldots,Ny}, R_{1z,2z,\ldots,Nz}, R_{(N+1)_y,(N+2)_y,\ldots,M_y},$$

$$R_{(N+1)_z,(N+2)_z,\ldots,M_z}\}^T$$

where (1,2,...,N) is the bearing node numbers related to nonlinearity while (N+1,N+2,...,M) is the other node numbers involving linear displacements which will be eliminated in the assembling procedure.

The housing coordinate vector can be rearranged in a similar fashion. After rearranging the coordinate vectors, the matrices $[M]_R, [M]_H, [C]_R, [C]_H, [K]_R$ and $[K]_H$, and other force vectors also need to be modified according to their vector components.

3.3a Computational harmonic balance method

Extending the procedure developed by Choi and Noah (1987), a steady state, a periodic solution for the motion of the rotor can be represented by a Fourier series expansion. For the displacement of the ith node, one writes

$$R_{iy} = A^i_{0y} + \sum_{n=1}^{N} \left(A^i_{ny} \cos \frac{n\omega t}{\nu} + B^i_{ny} \sin \frac{n\omega t}{\nu}\right) \tag{37a}$$

$$R_{iz} = C^i_{0z} + \sum_{n=1}^{N} \left(A^i_{nz} \cos \frac{n\omega t}{\nu} + B^i_{nz} \sin \frac{n\omega t}{\nu}\right) \tag{37b}$$

where ν is the subharmonic ratio, which is unity for harmonic and superharmonic cases, or an integer for subharmonic cases. Similar equations are written for the displacements H_{iy} and H_{iz} of the housing. Since the motion is periodic and steady state, the nonlinear coupling forces can also be written as

$$f_{iy} = C^i_{0y} + \sum_{n=1}^{N} \left(C^i_{ny} \cos \frac{n\omega t}{\nu} + D^i_{ny} \sin \frac{n\omega t}{\nu}\right) \tag{38a}$$

$$f_{iz} = C^i_{0z} + \sum_{n=1}^{N} \left(C^i_{nz} \cos \frac{n\omega t}{\nu} + D^i_{nz} \sin \frac{n\omega t}{\nu}\right) \tag{38b}$$

The nonlinear forces exerted on the housing are of equal and opposite sign to those of equations (38). To apply the harmonic balance method, one forms the vectors of the coefficients of $\cos \frac{n\omega t}{\nu}$ and $\sin \frac{n\omega t}{\nu}$, for n=1,2,...,N.

The constant coefficients of the displacements of the coupling forces are then written as follows:

For the constant term,

$$[K]_R \begin{pmatrix} \{A^0_m\} \\ \{A^0_s\} \end{pmatrix} = \begin{pmatrix} \{C^0_m\} \\ \{C^0_s\} \end{pmatrix} \tag{39}$$

where

$$\{A_m^0\} = \{A_{0y}^1, A_{0z}^1, \ldots, A_{0y}^N, A_{0z}^N\}^T$$

$$\{A_s^0\} = \{A_{0y}^{N+1}, A_{0z}^{N+1}, \ldots, A_{0y}^M, A_{0z}^M\}^T$$

$$\{C_m^0\} = \{C_{0y}^1, C_{0z}^1, \ldots, C_{0y}^N, C_{0z}^N\}^T$$

$$\{C_s^0\} = \{0, 0, 0, \ldots, 0, 0\}^T$$

and the subscripts of "m" and "s" stand for the master and slave part for a reduced algebraic system resulting from applying the harmonic balance method. The reduced out slave coordinates correspond to those coordinates where no nonlinear coupling forces exist. Therefore, the stiffness matrix of the rotor, $[K]_R$, is partitioned as

$$[K]_R = \begin{bmatrix} [K_{mm}]_R^{(2Nx2N)} & [K_{ms}]_R^{(2Nx2L)} \\ [K_{sm}]_R^{(2Lx2N)} & [K_{ss}]_R^{(2Lx2L)} \end{bmatrix}$$

where N is the total number of degrees of freedom at the nonlinearity and L is the total number of degrees of freedom associated with linear displacements of the rotor. Equation (39) is expanded as

$$[K_{mm}]_R\{A_m^0\} + [K_{ms}]_R\{A_s^0\} = \{C_m^0\} \tag{40a}$$

$$[K_{sm}]_R\{A_m^0\} + [K_{ss}]_R\{A_s^0\} = \{C_s^0\} \tag{40b}$$

Combining equations (39) and (40), the following equation is obtained

$$[[K_{mm}]_R - [K_{ms}]_R[K_{ss}]_R^{-1}[K_{sm}]_R]\{A_m^0\} = \{C_m^0\} \qquad (41)$$

By setting,

$$[\bar{K}]_R = [K_{mm}]_R - [K_{ms}]_R[K_{ss}]_R^{-1}[K_{sm}]_R, \qquad (2N \times 2N)$$

the final reduced matrix can be written as

$$[\bar{K}]_R\{A_m^0\} = \{C_m^0\} \qquad (42)$$

Because of the bearing clearances relations already given by equation (35), a discrete FFT algorithm will result in $\{C_m^0\}$ being a function of all the Fourier coefficients in equations (37) and the corresponding coefficients for the housing displacements. The implicit equation form of the relation (42) can be then expressed as

$$\{C_m^0\} = \{C_m^0\ (A_{0y}^N, A_{0z}^N, \ldots, A_{ny}^N, A_{nz}^N)\} \qquad (43)$$

where N is the total nonlinear degree of freedom number and n represents the retained harmonic terms. Newton-Rapshon (2nd order) iterative method is used, and for that purpose an incremental form is written in place of equation (42).

If one sets

$$\{A_m^0\} = \{A_m^0\} + \{\Delta A_m\}$$

$$\{C_m^0\} = \{C_m^0\} + \{\Delta C_m\}$$

then

$$[\bar{K}]_R\{\Delta A_m\} - \{\Delta C_m\} = \{C_m^0\} - [\bar{K}]_R\{A_m^0\} \tag{44}$$

This equation is solved sequentially with an equivalent set for the housing at each increment and iteration is used to obtain compatible coefficient increments for the rotor and housing.

Applying the harmonic balance method to the equations of motion (34), the cosine terms lead to

$$-(\frac{n\omega}{\nu})^2[M]_R\{A\} + (\frac{n\omega}{\nu})[C]_R\{B\} + [K]_R\{A\} = \{C_n\} + \{g_c\} \tag{45}$$

where

$$\{A\} = \{A_{ny}^1, A_{nz}^1, \ldots, A_{ny}^M, A_{nz}^M\}^T$$

$$\{B\} = \{B_{ny}^1, B_{nz}^1, \ldots, B_{ny}^M, B_{nz}^M\}^T \qquad (M = N+L)$$

$$\{C_n\} = \{C_{ny}^1, C_{nz}^1, \ldots, C_{ny}^N, C_{nz}^N, 0, 0, \ldots\ldots 0\}^T$$

$$\{g_c\} = \{0,0,0,\ldots,(me\omega^2)\gamma i, 0, (me\omega^2)\gamma j, 0, \ldots, 0\}^T$$

$$\text{if } n = \nu \quad (n=1,2,\ldots,N)$$

$$= \{0\} \qquad \text{if } n \neq \nu$$

where the γ's are the nodes at which the disks are located and M is the total node numbers and N is the node on which the nonlinear coupling forces of the rotor to the housing exist. Similar expressions are written for the housing.

For the sine terms, one obtains

$$-\left(\frac{n\omega}{\nu}\right)^2[M]_R\{B\} - \left(\frac{n\omega}{\nu}\right)[C]_R\{A\} + [K]_R\{B\} = \{D_n\} + \{g_s\} \qquad (46)$$

where

$$\{D_n\} = \{D^1_{ny}, D^1_{nz}, \ldots, D^N_{ny}, D^N_{nz}, 0, \ldots, 0\}^T$$

$$\{g_s\} = \{0,0,0,\ldots,(me\omega^2)\ ,0,(me\omega^2)\ ^j,0,\ldots,0\}^T$$

$$\text{if } n=\nu \quad (n=1,2,\ldots,N)$$

$$= \{0\} \qquad \text{if } n\neq\nu$$

Combining equations (45) and (46)

$$[S]_R\{Q\} = \{W\} + \{U\} \qquad (47)$$

where

$$\{W\} = \{C^N_{ny}, C^N_{nz}, D^N_{ny}, D^N_{nz}, 0, \ldots, 0\}^T$$

$$\{U\} = \{A^N_{ny}, A^N_{nz}, B^N_{ny}, B^N_{nz}, \ldots, B^M_{ny}, B^M_{nz}\}^T$$

To apply the reduction technique, equation (47) can be partitioned as follows.

$$\begin{bmatrix} [S_{mm}]_R^{(4Nx4N)} & [S_{ms}]_R^{(4Nx4L)} \\ [S_{sm}]_R^{(4Lx4N)} & [S_{ss}]_R^{(4Lx4L)} \end{bmatrix} \begin{pmatrix} \{Q_m\} \\ \{Q_s\} \end{pmatrix} = \begin{pmatrix} \{W_m\} \\ 0 \end{pmatrix} + \begin{pmatrix} \{U_m\} \\ \{U_s\} \end{pmatrix} \qquad (48)$$

where

$$\{Q_m\} = \{A^1_{ny}, A^1_{nz}, \ldots, B^N_{ny}, B^N_{nz}\}^T$$

$$\{Q_s\} = \{A^{N+1}_{ny}\ , A^{N+1}_{nz}\ , \ldots, B^M_{ny}, B^M_{nz}\}^T$$

$$\{W_m\} = \{C^1_{ny}, C^1_{nz}, \ldots, D^N_{ny}, D^N_{nz}\}^T$$

$$\{U_s\} = \{0, 0, \ldots, (me\omega^2)\gamma i, 0, 0, (me\omega^2)\gamma j, 0, \ldots, 0\}^T$$

$$\{U_m\} = \{0, 0, \ldots, 0, 0\}^T$$

Equation (48) can be expanded as

$$[S_{mm}]_R\{Q_m\} + [S_{ms}]_R\{Q_s\} = \{W_m\} + \{U_m\} \tag{49a}$$

$$[S_{ms}]_R\{Q_m\} + [S_{ss}]_R\{Q_s\} = \{U_s\} \tag{49b}$$

From equation (49b)

$$\{Q_s\} = [S_{ss}]^{-1}_R\{U_s\} - [S_{ss}]^{-1}_R[S_{ms}]_R\{Q_m\} \tag{50}$$

Combining equations (49a) and (50), the following equation is obtained.

$$\lfloor [S_{mm}]_R - [S_{ms}]_R[S_{ss}]^{-1}_R[S_{sm}]_R\{Q_m\} = \{W_m\} + \{U_m\}$$

$$- [S_{ms}]_R[S_{ss}]^{-1}_R\{U_s\}] \tag{51}$$

Set

$$[\bar{S}]_R = [S_{mm}]_R - [S_{ms}]_R[S_{ss}]^{-1}_R[S_{sm}]_R, \quad (4N \times 4N)$$

$$\{\bar{U}\} = [U_m] - [S_{ms}]_R[S_{ss}]^{-1}_R\{U_s\}, \quad (4N \times 1)$$

Equation (48) can then be rearranged as

$$[\bar{S}]_R\{Q_m\} = \{W_m\} + \{\bar{U}\} \tag{52}$$

To apply a numerical iteration procedure, one can use the following incremental form

$$\{Q_m\} = \{Q_m\} + \{\Delta Q_m\}$$

$$\{W_m\} = \{W_m\} + \{\Delta W_m\} \tag{53}$$

Substituting equation (53) into (52)

$$[\bar{S}]_R\{\Delta Q_m\} - \{\Delta W_m\} = \{W_m\} + \{\bar{U}\} - [\bar{S}]_R\{Q_m\} \tag{54}$$

Since the equation (54) is obtained only for one harmonic term, one can expand equation (54) for general retained harmonic terms

$$[\overline{S_n}]_R\{\Delta Q_{mn}\} - \{\Delta W_{mn}\} = \{W_{mn}\} + \{\overline{U_n}\} - [\overline{S_n}]_R\{Q_{mn}\}, \tag{55}$$

where $n = 1,2,\ldots,N$.

Equation (55) represents the cosine and sine incremental terms and equation (44) represents the incremental constant terms, so one can combine these equations. $\{Q_{mn}\}$ and $\{A_m\}$ contain the final solution forms which are solved by the Newton-Rapshon method. The overall incremental form for the rotor system will be as follows:

$$[T]_R\{\Delta r\} - \{\Delta v\} = \{z\} \tag{56}$$

where

$$\{\Delta r\} = \{\Delta A^1_{0y}, \Delta A^1_{0z}, \Delta A^2_{0y}, \Delta A^2_{0z}, \ldots, \Delta A^N_{0y}, \Delta A^N_{0z},$$

$$\Delta A^1_{1y}, \Delta A^1_{1z}, \Delta B^1_{1y}, \Delta B^1_{1z}, \ldots, \Delta B^N_{1y}, \Delta B^N_{1z},$$

$$\vdots$$

$$\Delta A^1_{ny}, \Delta A^1_{nz}, \Delta B^1_{ny}, \Delta B^1_{nz}, \ldots, \Delta B^N_{ny}, \Delta B^N_{nz}\}^T$$

$$\{\Delta\nu\} = \{\Delta C^1_{0y}, CA^1_{0z}, \Delta C^2_{0y}, \Delta C^2_{0z}, \ldots, \Delta C^N_{0y}, \Delta C^N_{0z},$$

$$\Delta C^1_{1y}, \Delta C^1_{1z}, \Delta D^1_{1y}, \Delta D^1_{1z}, \ldots, \Delta D^N_{1y}, \Delta D^N_{1z},$$

$$\vdots$$

$$\Delta C^1_{ny}, \Delta C^1_{nz}, \Delta D^1_{ny}, \Delta D^1_{nz}, \ldots, \Delta D^N_{ny}, \Delta D^N_{nz}\}^T$$

and

$$[T]_R = \begin{bmatrix} [\overline{K}]_R & \cdots & \cdots & 0 \\ 0^R & [\overline{S_i}]_R & \cdots & 0 \\ \vdots & \vdots & \ddots & \vdots \\ 0 & \cdots & \cdots & [\overline{S_n}]_R \end{bmatrix}$$

where

$$\{z\} = [\{C^0_m\} - [\overline{K}]_R\{A^0_m\}, \{W_{m1}\} - \{\overline{U_1}\} - [\overline{S_1}]_R\{\varsigma_{m1}\},$$

$$\{W_{m2}\} - \{\overline{U_2}\} - [\overline{S_2}]_R\{\varsigma_{m2}\}, \ldots,$$

$$\{W_{mn}\} - \{\overline{U_n}\} - [\overline{S_n}]_R\{\varsigma_{mn}\}]^T$$

$[\overline{K}]_R$ is (2N x 2N) and $[\overline{S_i}]_R$ is (4N x 4N) for (i = 1,2,...,n).

From equation (56), $\{\Delta v\}$ is written with partial derivatives of $\{\Delta r\}$. The partial derivative terms yield the Jacobian matrix, so one can finally obtain the following equation

$$\{\Delta v\} = [P]\{r\}' \tag{57}$$

where

$$[P] = \begin{bmatrix} \frac{\partial C^1_{0y}}{\partial A^1_{0y}} & \frac{\partial C^1_{0y}}{\partial A^1_{0z}} & \frac{\partial C^1_{0y}}{\partial A^2_{0y}} & \cdots & \frac{\partial C^1_{0y}}{\partial B^N_{nz}} \\ \frac{\partial C^1_{0z}}{\partial A^1_{0y}} & \frac{\partial C^1_{0z}}{\partial A^1_{0z}} & \frac{\partial C^1_{0z}}{\partial A^2_{0y}} & \cdots & \frac{\partial C^1_{0z}}{\partial B^N_{nz}} \\ \vdots & \vdots & \vdots & \ddots & \\ \frac{\partial D^N_{nz}}{\partial A^N_{nz}} & \frac{\partial D^N_{nz}}{\partial A^1_{0z}} & \frac{\partial D^N_{nz}}{\partial A^2_{0y}} & \cdots & \frac{\partial D^N_{nz}}{\partial B^N_{nz}} \end{bmatrix}$$

where the superscript stands for the degree of freedom number while subscript stands for the retained harmonic term in y or z direction.

The [P] matrix can be determined using numerical differentation of the discrete and inverse discrete FFT method. The matrix has to be updated at each iteration step until it converges. The steady state solution procedure for flexible housing is the same as for the rotor system as outlined above.

After calculating the rotor response using an iteration procedure, the coupling between rotor and housing are automatically calculated. These nonlinear coupling forces are then applied to the housing system to update the absolute housing

displacements and nonlinear coupling forces. Another iteration process is used to obtain once more the updated rotor response and then iterate until both rotor and housing responses have the same steady state convergent values.

3.3b Determination of multiple solutions: A global Newton's method

A method is further developed and adapted to rotor systems which is capable of locating all possible multiple solutions for the rotor's response. The method uses a double dogleg scheme (Dennis and Schnabel, 1979) with a local minimum algorithm to determine the solutions. A tunnelling method, developed by Levy et al. (1978) is further developed and used to remove the solutions already found from the formulation. Preliminary testing of the method showed the method to be capable of obtaining multiple solutions of the Duffing type equations.

An exposition of this method and preliminary results on its application will be published in due time.

4. NUMERICAL EXAMPLES AND DISCUSSION

4.1 Transient Response

The present convolution method is applied to a modified version of a rotor model constructed by Davis et al. (1984). The model was proposed to represent a simplified generic model of the space shuttle main engine turbopumps. The parameters and coefficients of the present generic model (shown in Fig. 5) are given in Tables 1 and 2. The imbalance forces are taken as shown in Fig. 5.

Response of the generic rotor-housing model at the bearing location is determined for the hypothetical start-up-shutdown case shown in Fig. 6. For the start-up case, from 0 to 0.01 seconds, using an increment of $1x10^{-5}$ sec., a comparison was made of the computer CPU time (on a VAX 8300) for the Runge-Kutta 4th order and the present convolution method (Fig. 7). It is seen that the hybrid convolution method is approximately twice as fast as the 4th order Runge-Kutta method. In addition, a desired accuracy can be met by the convolution method using a much larger time step than that required by the Runge-Kutta method.

Figs. 8-a and 8-b show the radial bearing force in bearing 1 for the linear and nonlinear (in presence of a clearance) cases, respectively, for the fast start-up of Fig. 6, 0-0.3 seconds. The initial conditions were taken as zero.

For the nonlinear cases, the radial force in bearing 1 has a peak close to $\dot{\phi}$ = 2600 rad/sec. (24830 rpm) during

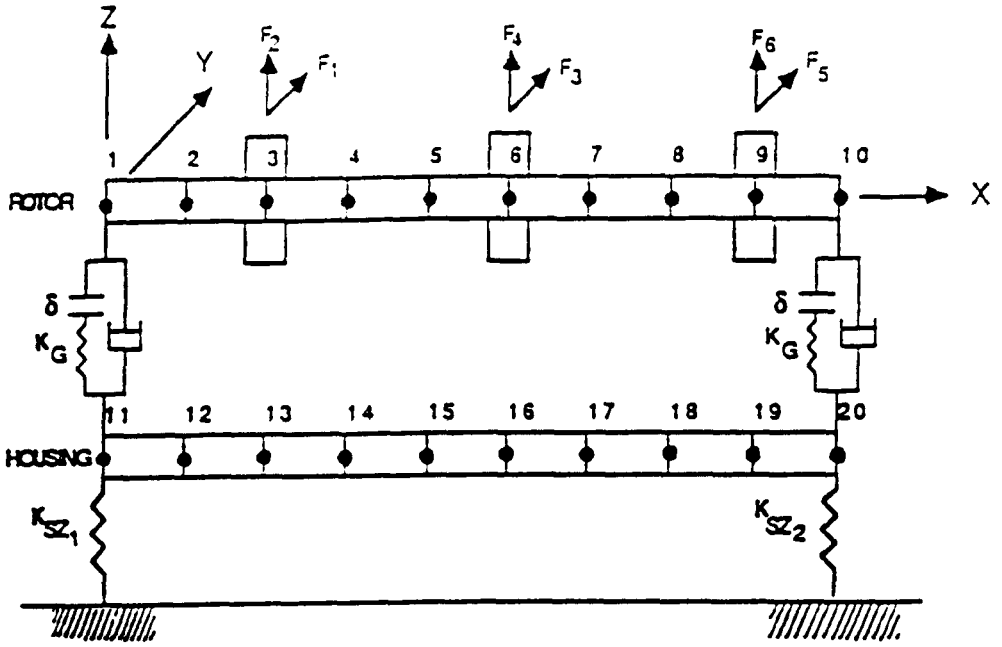

ROTOR: Shaft diameter: OD = 3.0 inches, ID = 0.0 inches
Material: Steel, $E = 3.0 \times 10^8$ psi
Joint length = 3.0 inches
Rotor length = 27.0 inches

HOUSING: Housing/Rotor weight ratio = 6/1

$(EI)_R = 1.1928 \times 10^8$ lb-in^3
$(EI)_H = 2.4 \times 10^8$ lb-in^3

$F_1(t) = m_1 e \dot{\phi}^2 \cos \phi t$ $\quad K_{SZ_1} = 4.0 \times 10^4$ lb/in
$F_2(t) = m_1 e \dot{\phi}^2 \sin \phi t$ $\quad K_{SY_1} = 5.0 \times 10^4$ lb/in
$F_3(t) = m_2 e \dot{\phi}^2 \cos \phi t$ $\quad K_{SZ_2} = 5.0 \times 10^4$ lb/in
$F_4(t) = m_2 e \dot{\phi}^2 \sin \phi t$ $\quad K_{SY_2} = 1.5 \times 10^5$ lb/in
$F_5(t) = m_3 e \dot{\phi}^2 \cos \phi t$ $\quad K_{BZ} = K_{BY} = 5.0 \times 10^5$ lb/in
$F_6(t) = m_3 e \dot{\phi}^2 \sin \phi t$ $\quad \delta = 5.0 \times 10^{-4}$ in

Figure 5. The generic model.

Table 1. Parameters of the Generic Model

	Mass ($lb\text{-}sec^2/in$)	Imbalance (in)	Moment of Inertia ($lb\text{-}in\text{-}sec^2$)	
			Polar	Diametrical
Disk 1	0.0259	0.002	0.028	0.0159
Disk 2	0.0389	0.002	0.193	0.101
Disk 3	0.0518	0.002	1.0057	0.5078

Table 2. Coefficients of the Generic Model

	K_{YY} K_{ZZ} (lb/in)	$K_{XY} = K_{YX}$ (lb/in)	C_{YY} C_{ZZ} (lb-sec/in)	Side Force (lb)	
				Y-direction	Z-direction
DISK 1	1.0×10^5	1.5×10^4	6.3×10^1	$4.95 \times 10^{-6}\ \dot{\phi}^2$	$-2.806 \times 10^{-5}\ \dot{\phi}^2$
DISK 2	-8.9×10^3	-4.0×10^3	1.0	$6.117 \times 10^{-5}\ \dot{\phi}^2$	$7.281 \times 10^{-5}\ \dot{\phi}^2$
DISK 3	8.7×10^3	1.9×10^3	2.3	$2.379 \times 10^{-5}\ \dot{\phi}^2$	0

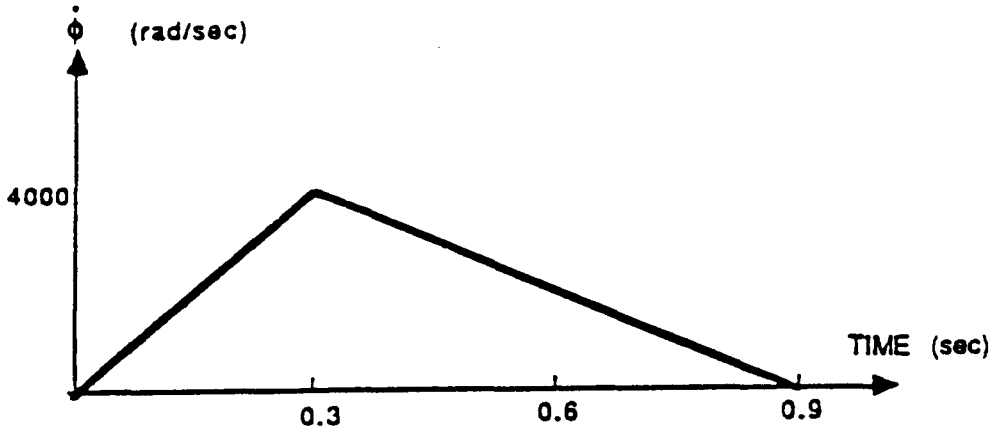

Figure 6. Running speed of rotor.

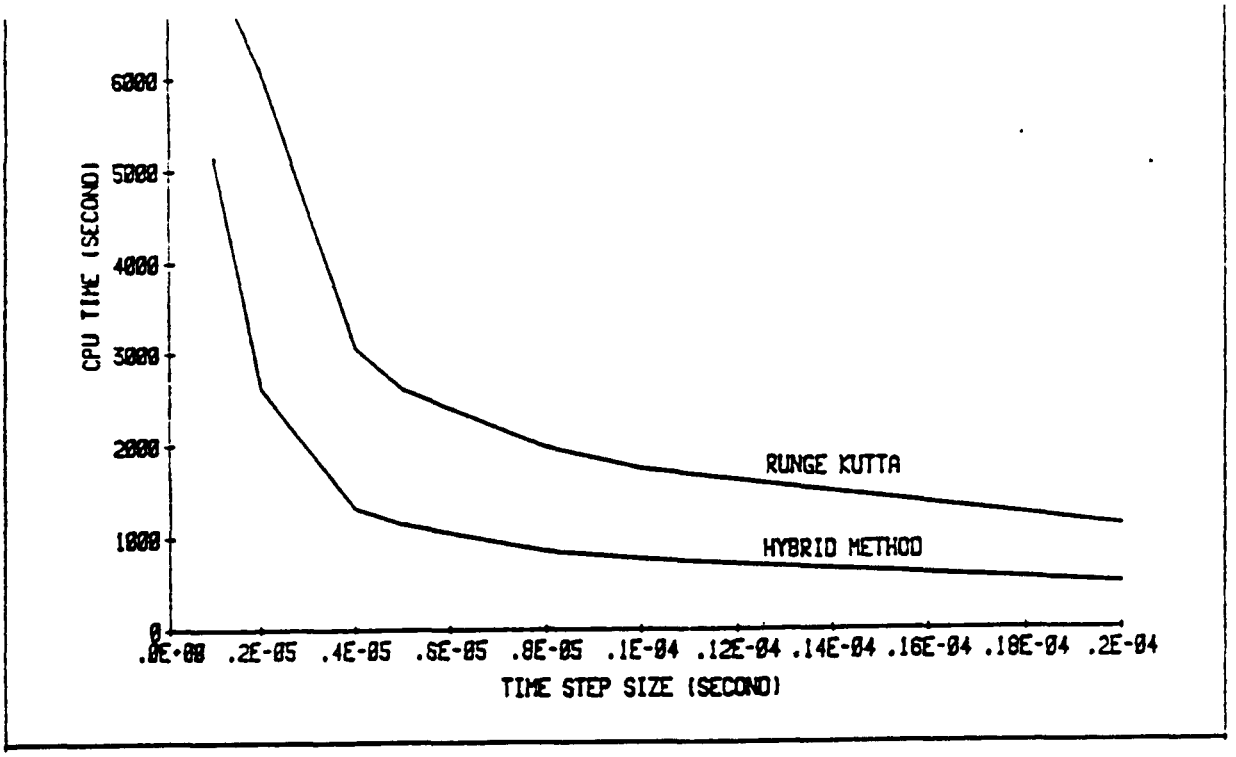

Figure 7. CPU plot of hybrid method and Runge Kutta method.

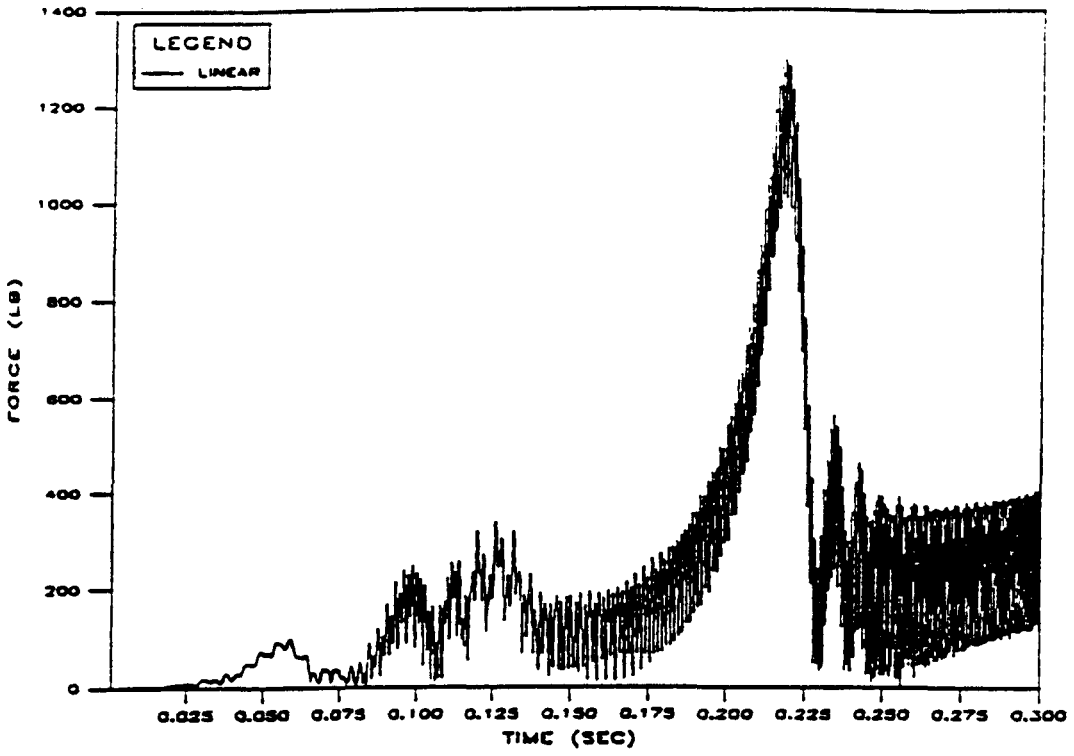

Figure 8a. Force in linear bearing 1 (δ = 0).

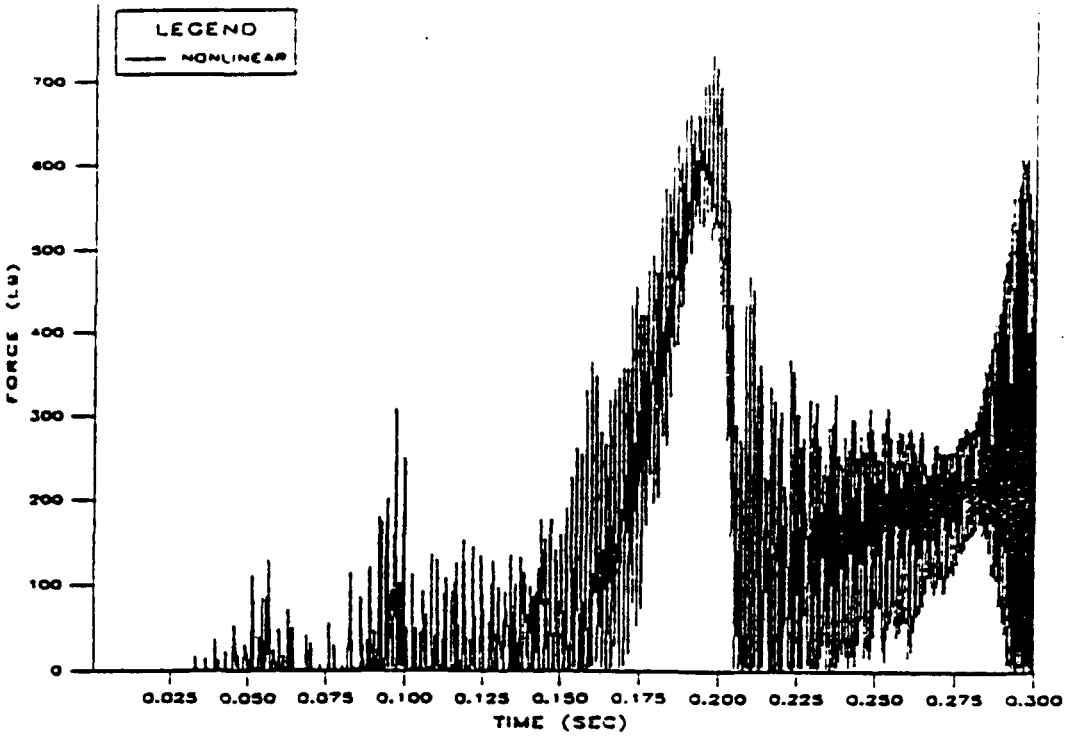

Figure 8b. Force in nonlinear bearing 1 (δ = 5×10^{-4} in).

start-up and a much higher peak at $\dot{\phi}$ = 3560 rad/sec. (34000 rpm) during the (slower) shutdown in Fig. 9. The linear system with zero bearing clearances shows higher bearing load peaks than with the nonlinear system. In the linear case, the load peak occurs, as expected, at the critical speed. For the nonlinear cases other results, not shown here, show that the bearing forces at bearing 2 are consistently higher than those at bearing 1.

Figs. 10-a and 10-b show the Y-displacements of the rotor relative to the housing at bearing 1 for the start-up conditions for the linear and nonlinear cases, respectively.

4.2 Periodic Response

The harmonic balance/FFT method was used to generate forced nonlinear periodic responses of the generic model (Fig. 5) in the range of 0-40,000 rpm. Figure 11 shows the fundamental synchronous responses at the two critical speeds to occur around 1900 rad/sec an 4300 rad/sec. The figure shows the radial displacements of the rotor relative to the housing at the left bearing. The critical speed map is depicted in Figure 12 for the generic model in absence of bearing clearances. The gyroscopic terms are included which are shown to raise the forward critical speeds and lower the backward critical speeds. The figure shows the first two critical speeds to

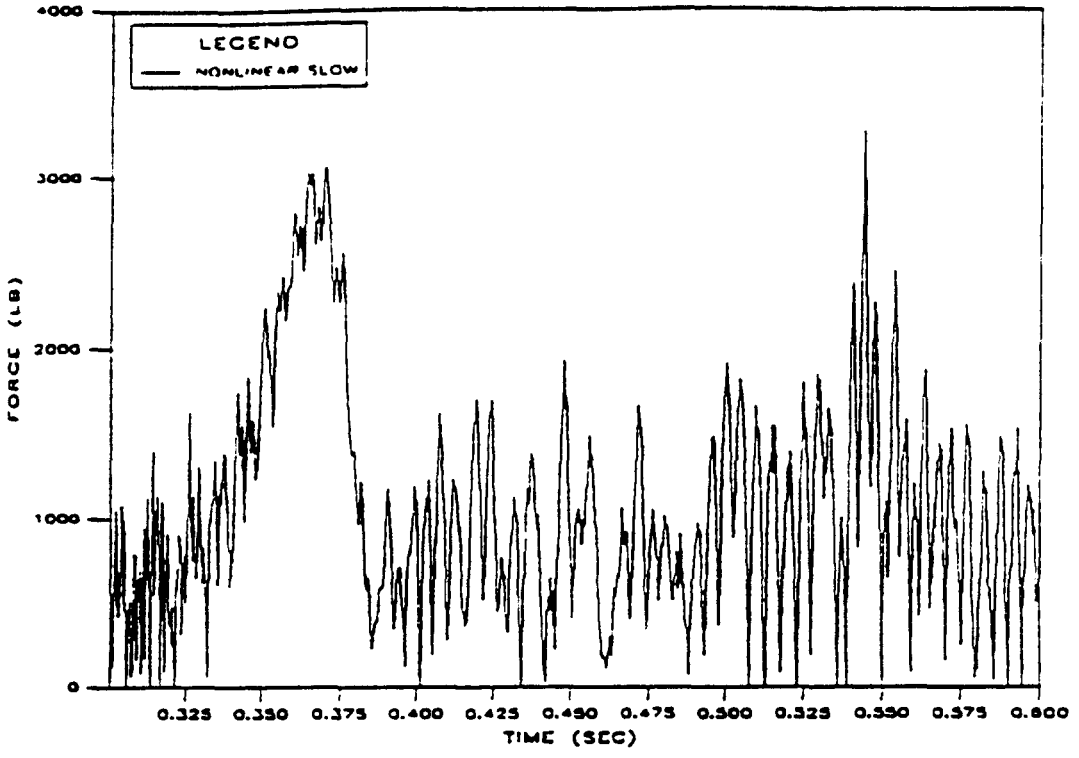

Figure 9. Force in nonlinear bearing 1 during shutdown.

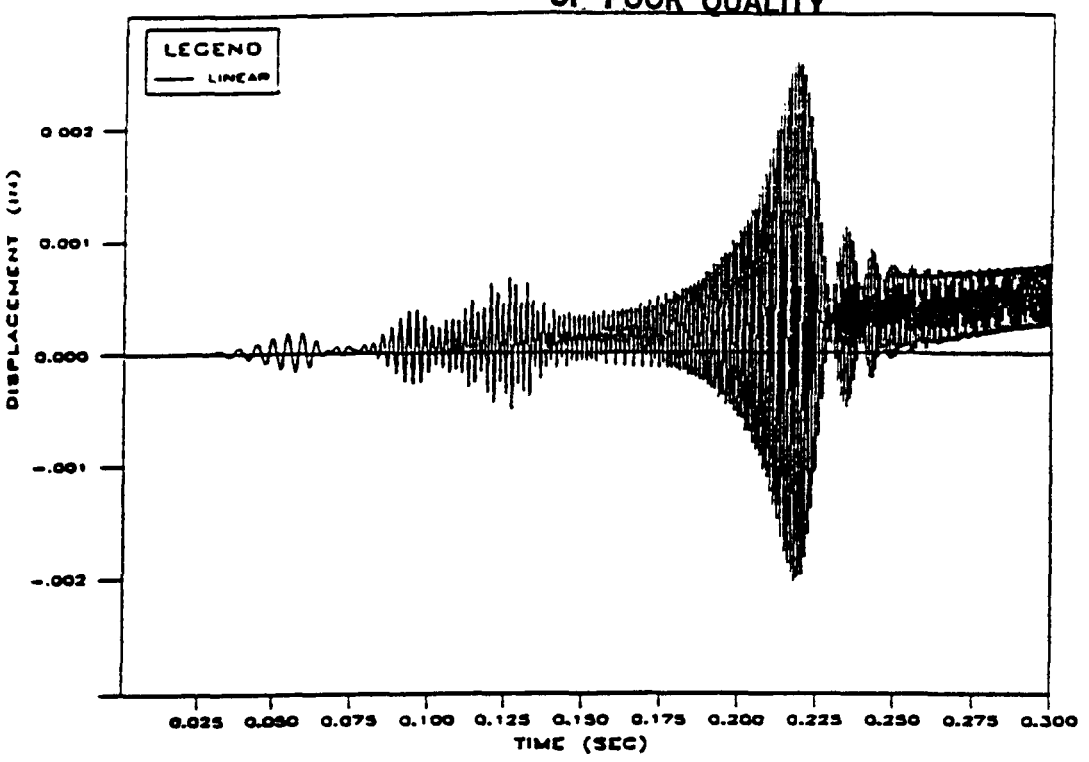

Figure 10a. Relative displacement of rotor in Y-direction at linear bearing 1.

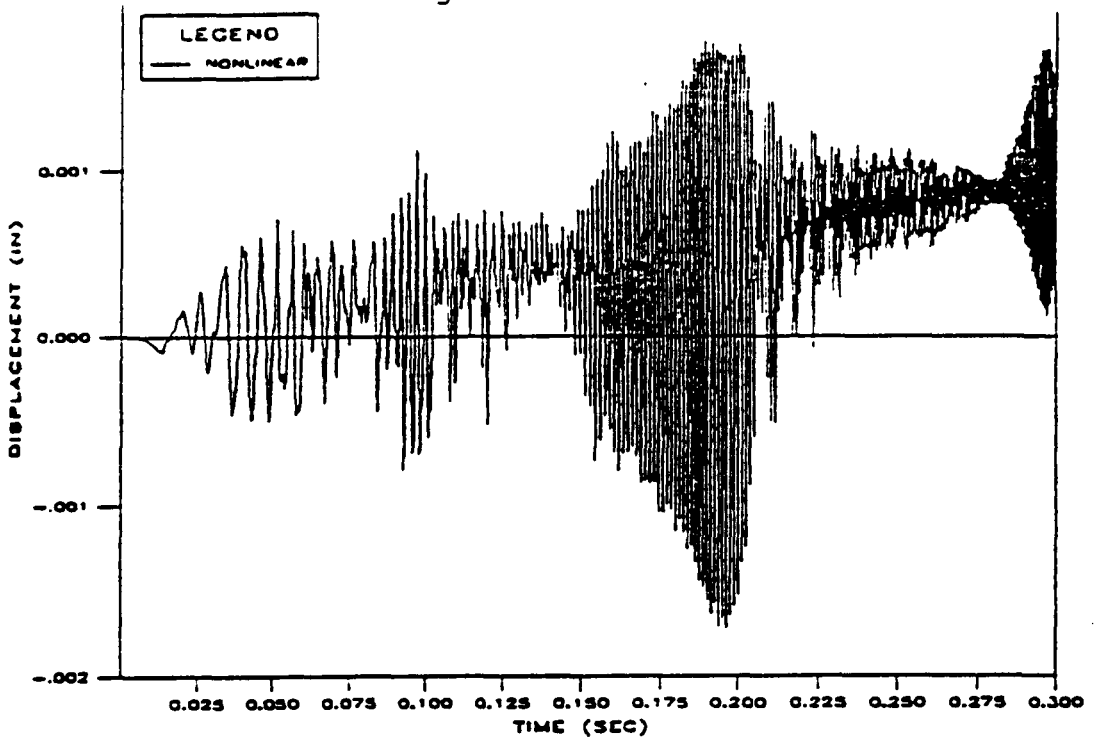

Figure 10b. Relative displacement of rotor in Y-direction at nonlinear bearing 1.

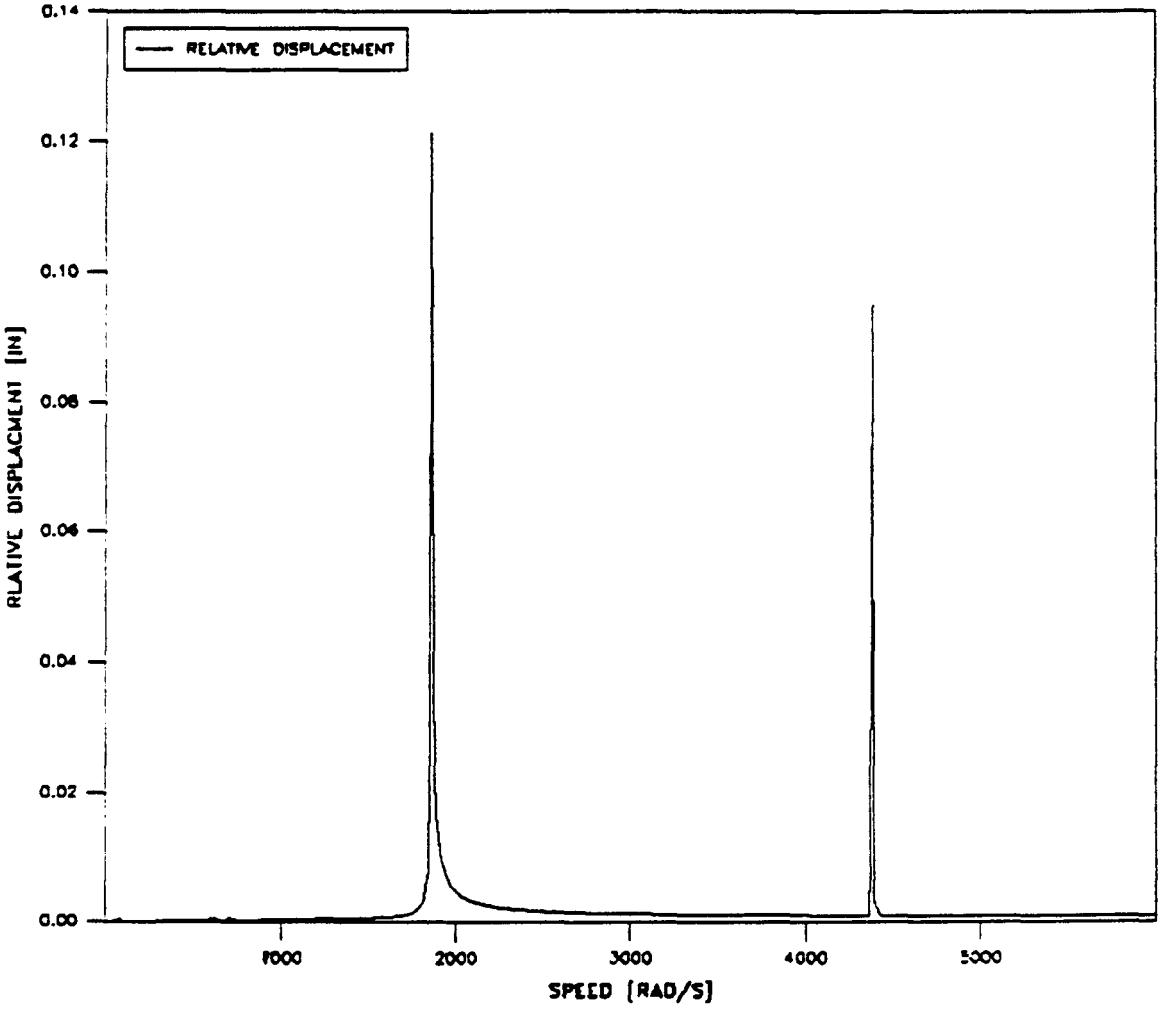

Figure 11. Critical speed of linear generic model at bearing 1; eccentricity = 0.5 mils, no damping, no gyroscopic effects.

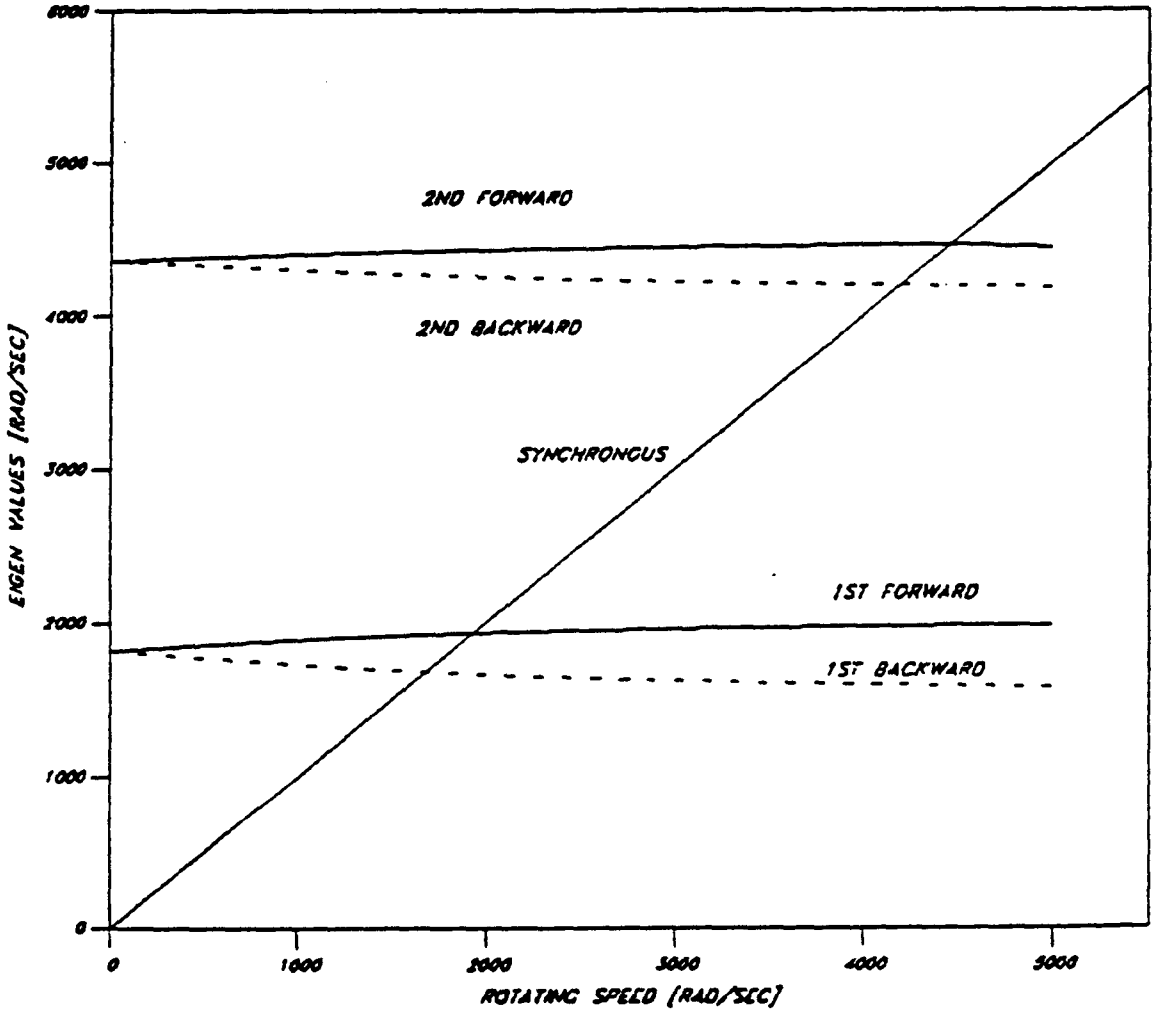

Figure 12. Critical speed map for the linear generic model; no damping.

be exactly the same as those of the linear case obtained using the harmonic balance/FFT method. Numerical calculation is performed to investigate the existence of subharmonic responses.

The trajectory of the shaft center of a 1/n order subharmonic response lies in the region bounded by circles with radii which are determined by the harmonic and subharmonic amplitudes. The trajectory touches the bounded circles at (n-1) points for forward whirl and (n+1) points for backward whirl (See Tondl, 1973). The shaft center trajectory is studied to identify the subharmonic responses and to compare the amplitude between the harmonic response and the 1/n order subharmonic response with various values of the side force, gap size and eccentricity near the critical speeds. To allow the occurrence of the subharmonic response, the damping is set to a small value for all cases. The results are shown in Figures 13, 14, 15 and 16. These figures show that all subharmonic responses occur around the second critical speed and that all are of the 1/2 order. In Figure 13, the harmonic and subharmonic amplitudes are almost of the same magnitude for a small side force. In Figure 14, the harmonic response becomes dominant when reducing the bearing clearance size. On the contrary, the 1/2 order subharmonic response becomes larger than the amplitude of the harmonic component by increasing the clearance size as can be seen in Figure 15. The gap size has a significant effect on the existence of the 1/2 order subharmonics in the HPOTP model

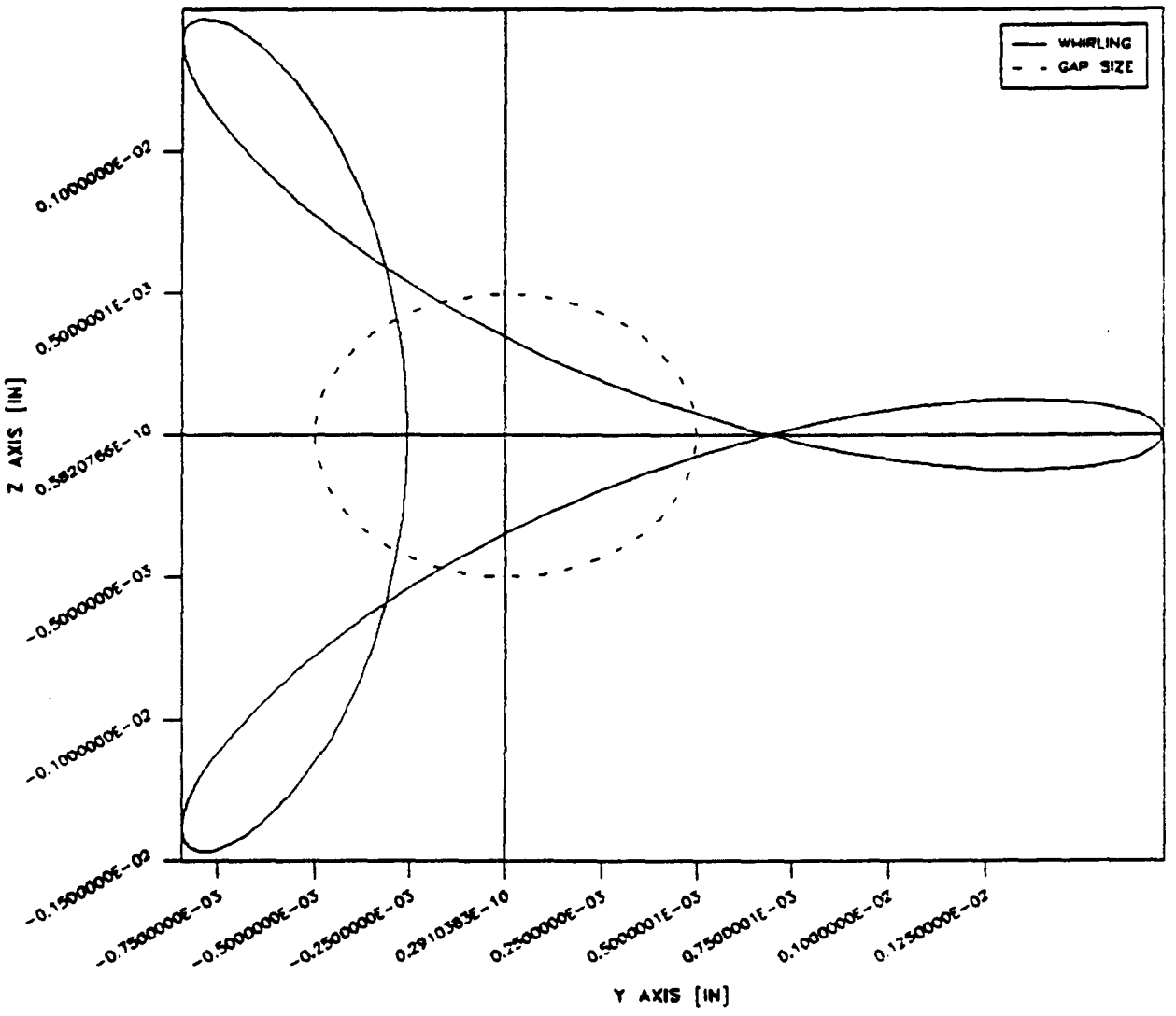

Figure 13. Trajectory for subharmonic motion of order 1/2; gap = 0.5 mils, eccentricity = 0.5 mils, side force = 10 lbs., speed = 4210 rad/sec.

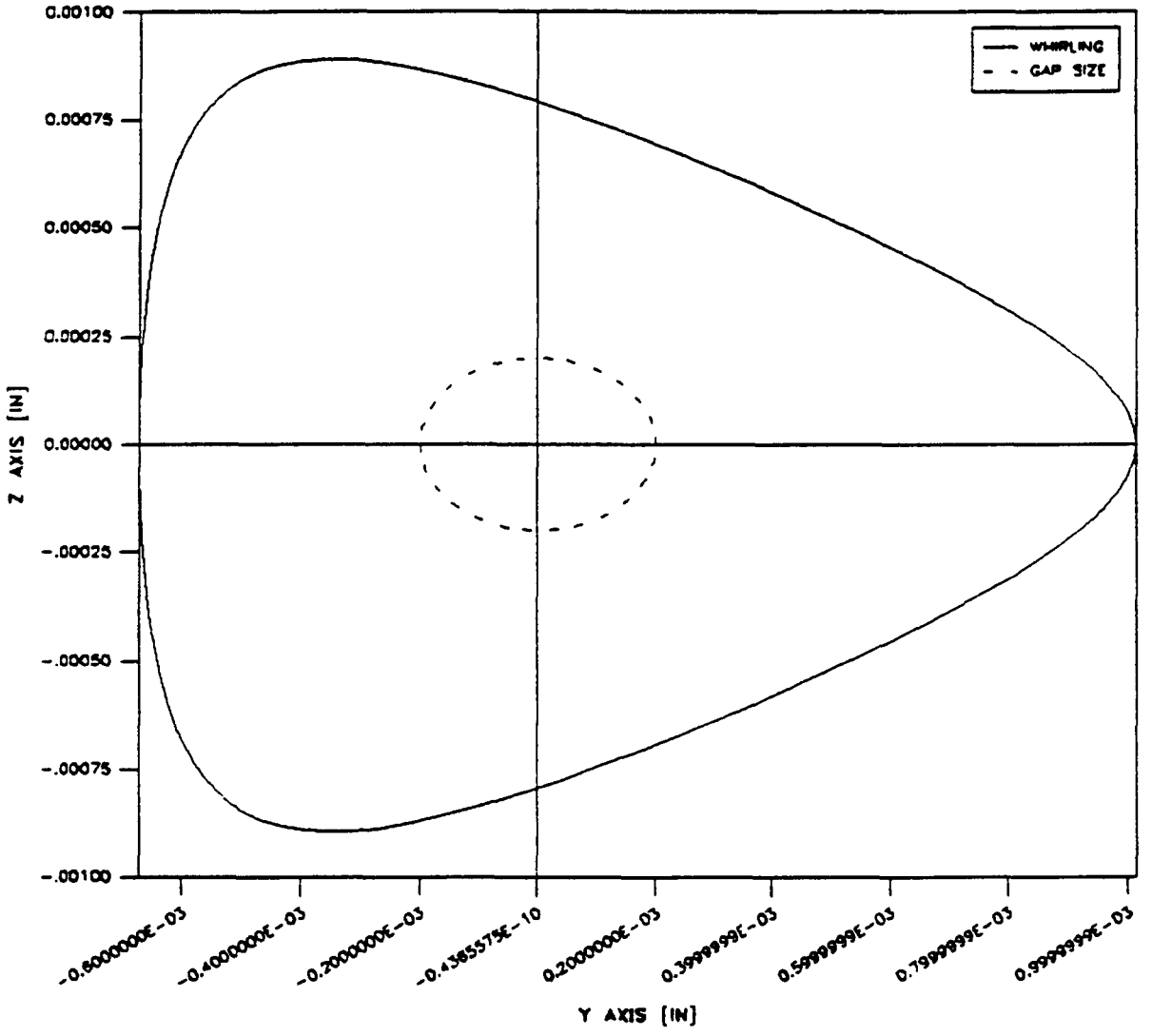

Figure 14. Trajectory for subharmonic motion of order 1/2; gap = 0.2 mils, eccentricity = 0.5 mils, side force = 10 lbs., speed = 4210 rad/sec.

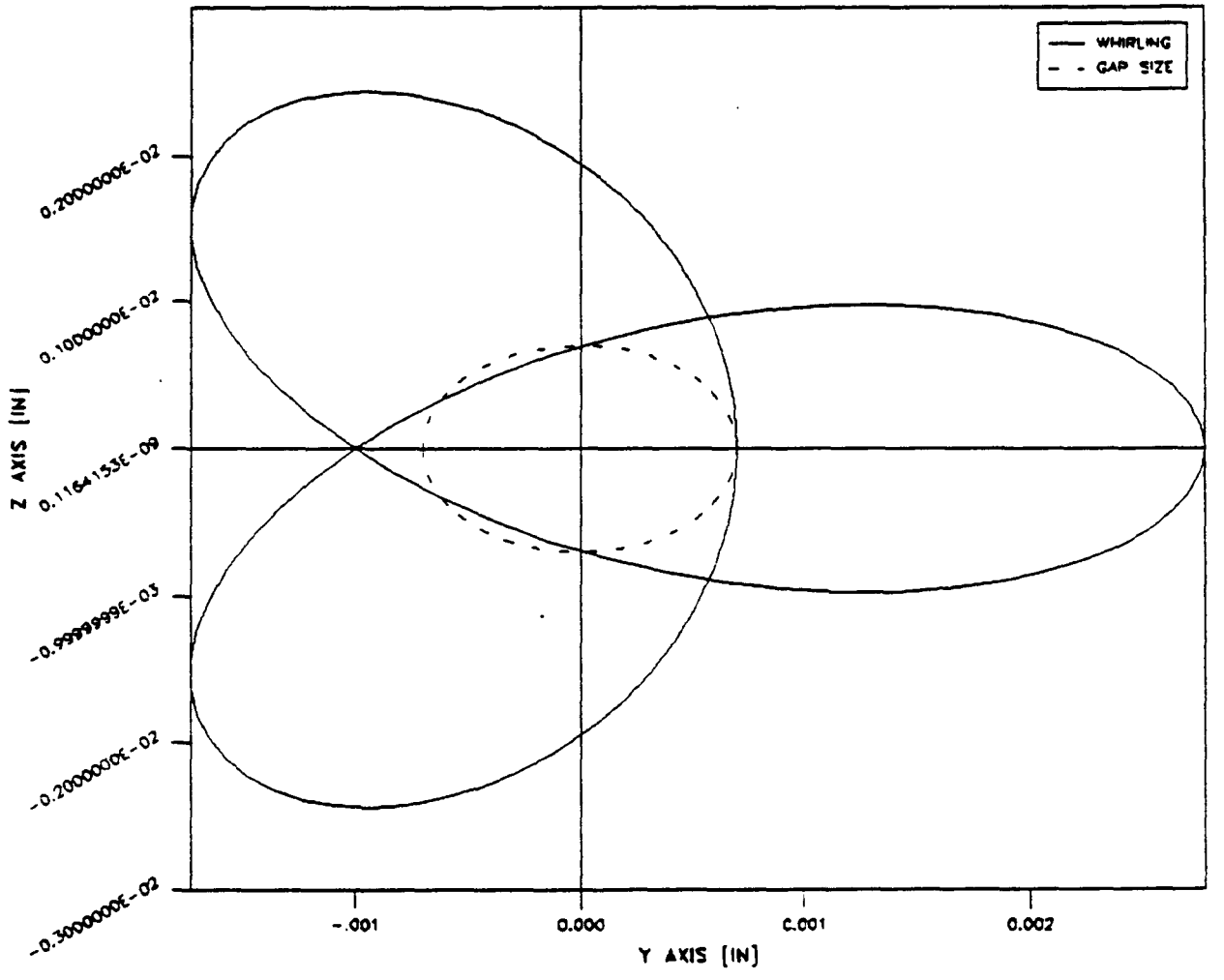

Figure 15. Trajectory for subharmonic motion of order 1/2; gap = 0.7 mils, eccentricity = 0.5 mils, side force = 10 lbs., speed = 4210 rad/sec.

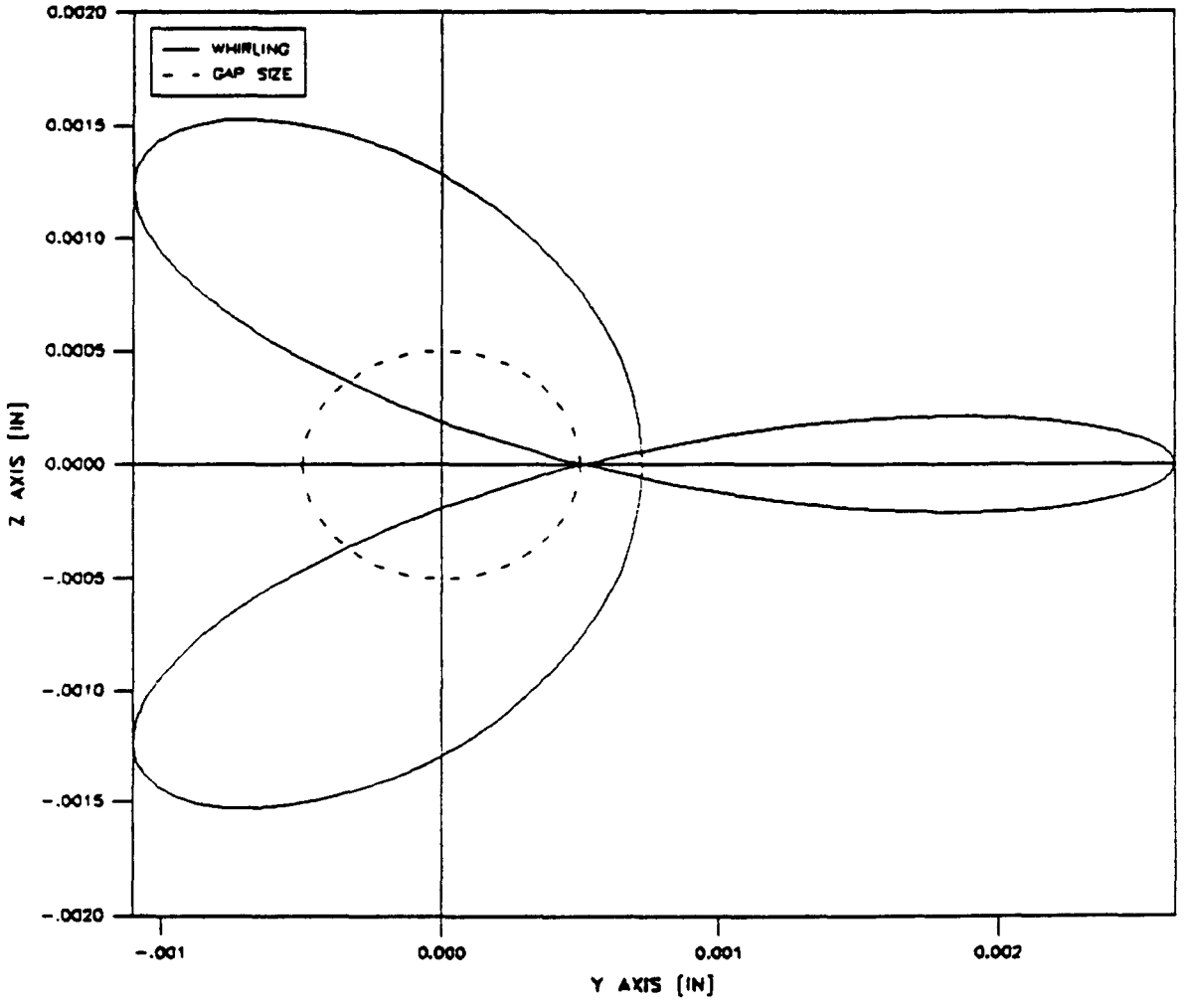

Figure 16. Trajectory for subharmonic motion of order 1/2; gap = 0.5 mils, eccentricity = 0.5 mils, side force = 100 lbs., speed = 4210 rad/sec.

regardless of the side force. In Figure 16, the side force is raised to ten times that of Figure 13. In that case, the results show the amplitude of the subharmonic response becoming slightly larger than the harmonic response. This result reveals that the side force also has some influence on whether any subharmonic response occurs.

More detailed investigation comparing the effects of the side force and gap size is studied and the results are shown in Figure 17. The figure shows that the side force has a significant effect on the existence of the 1/2 order subharmonic response. Around 200 lbs. side force and 0.5-0.7 mils of gap size is the region which induces the large amplitude of the 1/2 order subharmonic. Excessive side force, larger than 400 lbs. will cause a reduction of the subharmonic responses. With constant gap size and eccentricity, there exists a certain range of side force region in which larger subharmonic response would occur. This agrees with results presented by Choi and Noah (1987).

The effect of eccentricity on the existence of the 1/2 order subharmonic response with variation of the side force is shown in Figure 18. The figure shows that the eccentricity has the effect of shifting the location of the maximum subharmonic response to the right. The side force ranges at which the maximum 1/2 order subharmonic response occurs are different for each eccentricity. The figure also shows that the larger eccentricity is the lower the subharmonic response will be.

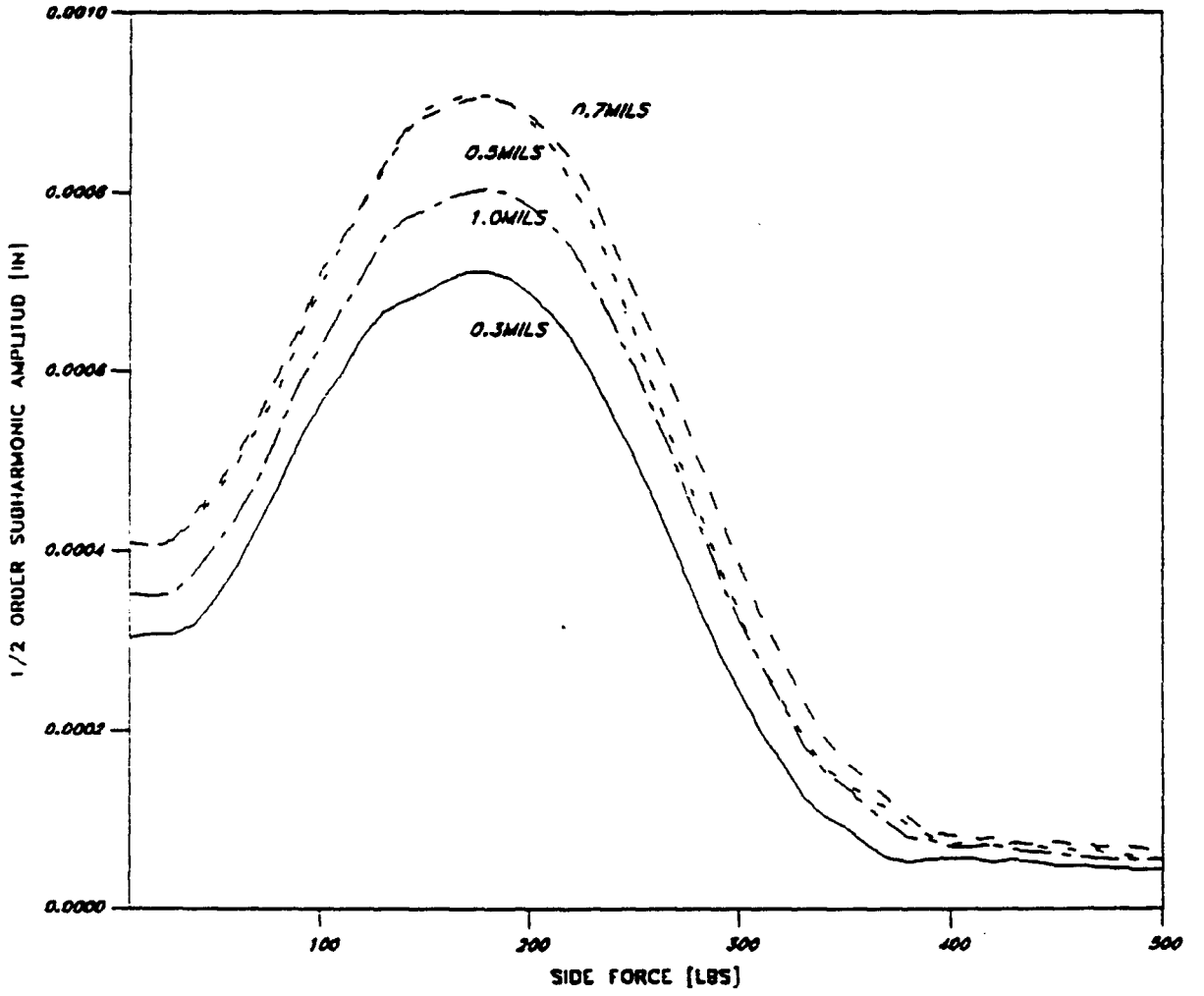

Figure 17. Gap size effect on subharmonic motion of order 1/2; eccentricity = 0.5 mils, speed = 4210 rad/sec.

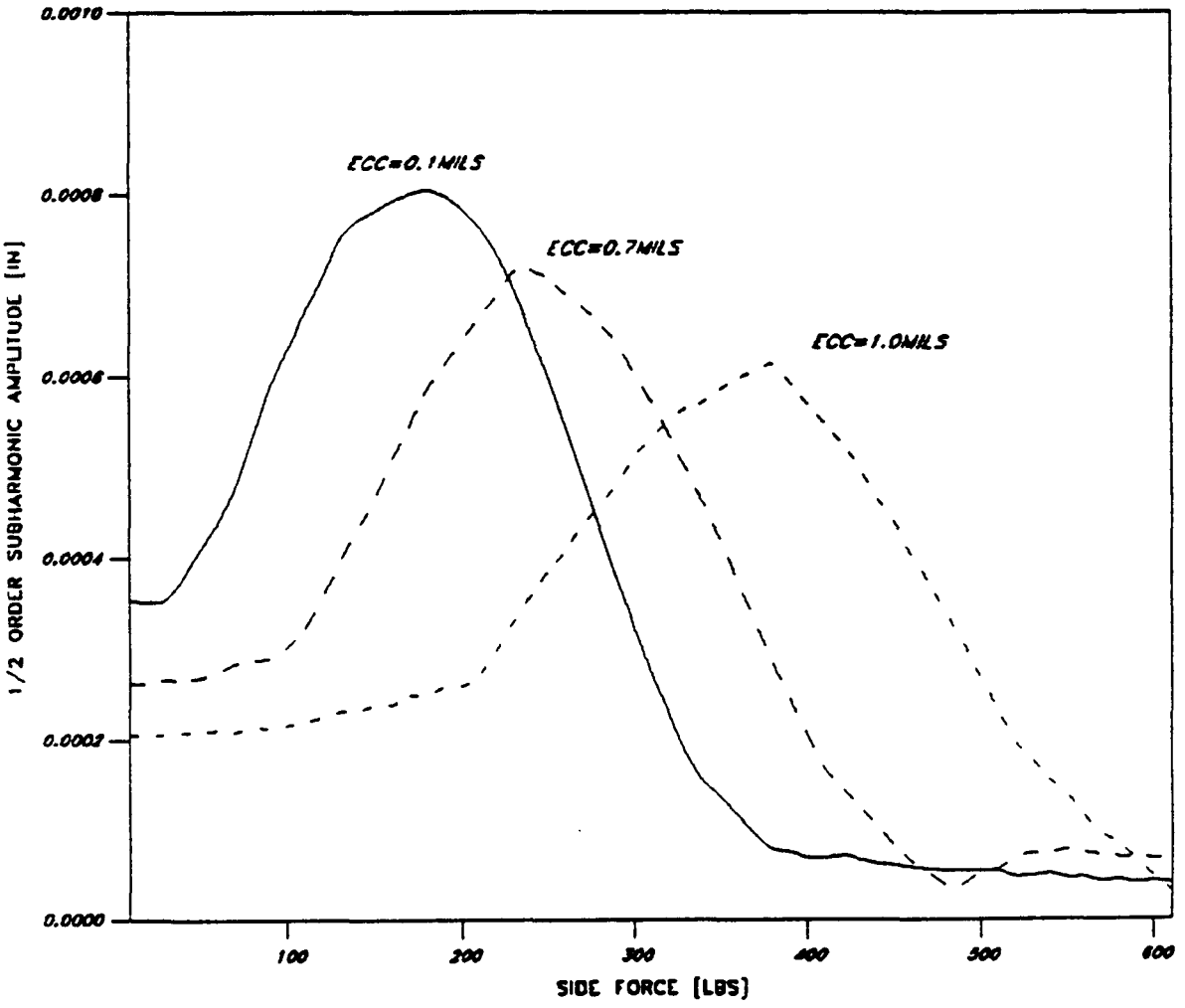

Figure 18. Mass eccentricity effect on subharmonic motion of order 1/2; gap size = 0.5 mils, speed = 4210 rad/sec.

This may be explained by the fact that larger response amplitude due to larger eccentricity induces more contact causing the system to become relatively weakly nonlinear resulting in a lesser subharmonic amplitude. It may therefore be necessary to reduce the gap size and side forces in any proposed design or maintainance criteria in order to eliminate dangerous subharmonic responses.

5. CONCLUSIONS AND RECOMMENDATIONS

5.1 Conclusions

The hybrid convolution approach developed in this study is shown to provide an efficient closed form integral formulation for determining the transient response of linear systems coupled through local nonlinearities. A typical application in which the present method proved quite effective is the determination of the transient response of a generic model of the high pressure oxygen turbopump (HPOTP) of a space shuttle main engine (SSME) in presence of bearing clearances, constituting the local nonlinearities. Substantial savings in computation time were achieved as compared with direct numerical integration techniques.

The use of the transition matrix allows the representation of rotors involving skew-symmetric matrices of gyroscopic loads or other nonconservative systems with general velocity coefficient matrices. A Duhamel integral would represent quite effectively other systems with classical modes, such as the housing of the HPOTP or other nonrotating, proportionally damped structures. The convolution formulation allows accommodating with ease changes in the nonlinear or linear coupling parameters among the various linear subsystems involved.

Possible improvement of the method could be achieved through replacement or optimization of the iteration procedure utilized in this study.

The results shown here show that the presence of bearing clearance can drastically alter the rotor response in the HPOTP. As noted by Ishida et al. (1987) for a simpler system, it is more difficult to go through a critical speed in the presence of the nonlinearity.

An effective numerical harmonic balance algorithm for determining the steady-state forced vibration of a highly nonlinear multi degree-of-freedom rotor system has been developed. The results show that the method is computationally superior to that of any direct numerical integration method. In addition, the complicated nonlinear steady-state periodic motions of multi degree-of-freedom rotor systems can readily be studied using the present method.

It is shown that dangerous subharmonic resonances may occur for the HPOTP in the presence of bearing clearances, mass eccentricities, and fluid side forces. The results show that the ranges of the above three parameters are mutually related in influencing the subharmonic occurrence. In particular, the bearing clearance size to shaft amplitudes at the bearing, the local stiffness at the bearings, and the side forces, were found to highly influence the degree of nonlinearity in the rotor system and therefore determine its response and stability.

5.2 Recommendations

It is recommended that future studies should include the following:

1. Represent rotor and housing models in terms of their linear modal coordinates as utilized in the turbopumps of the SSME.
2. Develop computational-Floquet or alternative analysis techniques for determining the stability of the periodic synchronous and subsynchronous response of rotor-housing systems. Further refine the computational harmonic balance method for achieving more controlled accuracy, particularly within the resonance parameter regions.
3. Develop method for determining the aperiodic response and criteria for detecting onset of probable chaotic motions.
4. Perform extensive parametric studies of the steady state (periodic, aperiodic and chaotic) and transient responses of the actual SSME turbopumps to completely characterize their dynamic behavior for existing and proposed design modifications.

ACKNOWLEDGEMENT

This work was carried out as part of a research project supported by NASA, Marshall Flight Center, under contract No. NAS8-36293. The author and co-research assistants are grateful to Thomas Fox, the technical monitor, for his enthusiastic support and interest.

REFERENCES

Adams, M.L., 1980, "Non-Linear Dynamics of Flexible Multi-Bearing Rotors," Journal of Sound and Vibration, Vol. 71, pp. 129-144.

Beatty, R.F., 1985, "Differentiating Rotor Response Due to Radial Rubbing," ASME Journal of Vibration, Acoustics, Stress, and Reliability in Design, Vol. 107, pp. 151-160.

Bently, D., 1979, "Forced Subrotative Speed Dynamic Action of Rotating Machinery," ASME paper No. 74-ET-16, Petroleum Mechanical Engineering Conference, Dallas, Texas.

Cipra, R.J., and Uicker, J.J., Jr., 1981, "On the Dynamic Simulation of Large Nonlinear Mechanical Systems, Part 1: An Overview of the Simulation Technique. Substructuring and Frequency Domain Considerations," ASME J. of Mechanical Design, vol. 103, pp. 849-865.

Childs, D.W., 1978, "The Space Shuttle Main Engine High Pressure Fuel Turbopump-Rotordynamic Instability Problem," ASME Journal of Engineering for Power, Vol. 100, pp. 48-51.

Childs, D.W., 1982, "Fractional-Frequency Rotor Motion due to Nonsymmetric Clearance Effects," ASME Journal of Energy and Power, Vol. 104, pp. 533-541.

Childs, D.W. and Moyer, D.S., 1984, "Vibration Characteristics of the HPOTP (High Pressure Oxygen Turbopump) of the SSME (Space Shuttle Main Engine), ASME Paper No. 84-GT-31, International Gas Turbine Conference, Amsterdam, Netherlands, June.

Choi, Y.S., and Noah, S.T., 1987, "Nonlinear Steady-State Response of a Rotor Support System," ASME Journal of Vibration, Acoustics, Stress, and Reliability in Design, Vol. 109, pp. 255-261.

Choi, Y.S. and Noah, S.T., 1988, "Forced Periodic Vibration of Unsymmetric Piecewise-Linear Systems," J. Sound and Vibration, Vol. 120, No. 3.

Clough, R.W. and Wilson, E.L., 1979, "Dynamic Analysis of Large Structural Systems with Local Nonlinearities," Computer Methods in Applied Mechanics and Engineering, Vol. 17/18, pp. 107-129.

Davis, L.B., Wolfe, E.A., Beatty, R.F., 1984, "Housing Flexibility Effects on Rotor Stability," MSFC Advanced High Pressure O_2/H_2 Technology Conf. Proceedings, G. Marshall Space Flight Center, Huntsville, Alabama.

Day, W.B., 1987, "Asymptotic Expansions in Nonlinear Rotordynamics," Quarterly of Appl. Math., Vol. XLIV, No. 4, pp. 779-792.

Dennis, J.E., Jr., and Schnabel, R.B., 1979, Quasi-Newton Methods for Unconstrained Nonlinear Problems, Short Course on Modern Computational Techniques for Nonlinear Unconstrained Optimization, Madison, Wisconsin.

Ehrich, F.F., 1966, "Subharmonic Vibrations of Rotors in Bearing Clearance," ASME paper No. 66-MD-1, Design Engineering Conference and Show, Chicago, Ill., May 9-12.

Fan, U.J., and Noah, S.T., "Vibration Analysis of Rotor Systems Using Reduced Subsystem Models," To appear in the AIAA Journal of Propulsion and Power.

Glease, J.R. and Bukley, P., 1984, "Effect of Bearing Deadbands on Bearing Loads and Rotor Stability," MSFC Advanced High Pressure O_2/H_2 Technology Conference Proceedings, G. Marshall Space Flight Center; Huntsville, Alabama, June 27-29.

Ishida, Y., Ikeda, T. and Yamamoto, T., 1987, "Transient Vibration of a Rotating Shaft with Nonlinear Spring Characteristics During Acceleration through a Major Critical Speed," JSME Int. J., Vol. 30, No. 261, pp. 458-466.

Kubomura, K., 1985, "Transient Loads Analysis by Dynamic Condensation," ASME J. Applied Mechanics, Vol. 52, pp. 559-564.

Levy, A.V., Montalvo, A., Gomez, S., and Calderon, A., 1978, "Topics in Global Optimization," in Lecture Notes in Mathematics, Note #909, pp. 18-33, Springer-Verlag, Berlin Heidelberg, New York.

Meirovitch, L., 1980, Computational Methods in Structural Dynamics, Sijthoff and Noordhoff.

Muszynska, A., 1984, "Partial Lateral Rotor to Stator Rubs," Proceedings of the I. Mech. E. 3rd. Intl. Conf. on Vibrations in Rotating Machinery, Univ. of York, 11-13 Sept., pp. 327-335.

Nataraj, C., and Nelson, H.D., 1987, "Periodic Solutions in Rotor Dynamic Systems with Nonlinear Supports: A General Support," ASME Design Conference, Oct.

Neilson, R.D., and Barr, A.D.S., 1988, "Response of Two Elastically Supported Rigid Rotors Sharing a Common Discontinuously Nonlinear Support," Proceedings of the Institution of Mechanical Engineers, Heriot-Watt University, 13-15 Sept., pp. 589-598.

Nelson, H.D., Meacham, W.L., Fleming, D.P. and Kascak, A.F., 1982, "Nonlinear Analysis of Rotor Bearing Systems Using Component Mode Synthesis," ASME Paper No. 82-GT-303.

Noah, S.T., 1984, "Rotordynamic Analysis of the SSME Turbopumps Using Reduced Models," Final Report on NASA Contract NAS8-34505, Texas A&M University, Sept.

Noah, S.T., 1986, "Hybrid Methods for Rotordynamic Analysis," Final NASA Report, G.C. Marshall Space Flight Center, Alabama, under contract No. NAS8-36182, December 1986.

Noah, S.T., Chiang, I.F. and Kim, Y.B., 1988, "Dynamic Analysis of Nonlinear Rotor/Housing Systems," MSFC Advanced High Pressure O_2/H_2 Technology Conf. Proceedings, G. Marshall Space Flight Center, Huntsville, Alabama.

Noah, S.T., Fan, U.J., Choi, Y.-S., and Fox, T., 1986, "Efficient Transient Analysis Methods for the Space Shuttle Main Engine Turbopumps," NASA Conf. on Advanced Earth-to-Orbit Propulsion Tech., G. Marshall Flight Center, Huntsville, Alabama, May 13-15.

Nordmann, R., 1975, "Eigenvalues and Resonance Frequency Forms of Turborotors with Sleeve Bearings Crank Excitation, External and Internal Damping," Machine Dynamics Group, Technical University Darmstadt, West Germany, June 1975.

Saito, S., 1985, "Calculation of Nonlinear Unbalance Response of Horizontal Jeffcott Rotors Supported by Ball Bearings with Radial Clearances," ASME paper No. 85-DET-33.

Shaw, S. and Holmes, P.J., 1983, "A Periodically Forced Piecewise Linear Oscillator," J. Sound Vib., Vol. 90, pp. 129-155.

Tondl, A., 1965, Some Problems of Rotor Dynamics, Chapman and Hall, London, 1965.

Tondl, A., 1973, "Notes on the Identification of Subharmonic Resonances of Rotors," Journal of Sound and Vibration, Vol. 31, No. 1, pp. 119-127.

Tongue, B.H. and Dowell, E.H., 1983, "Component Mode Analysis of Nonlinear, Nonconservative Systems," ASME Journal of Appl. Mech., Vol. 50, pp. 204-209.

Von Pragenau, G.L., 1981, "Large Step Integration for Linear Dynamic Systems," Conference Proc. IEEE Southeastern '81, reprint, April.

Yamamoto, T.T., 1954, "On Critical Speeds of a Shaft," Memoirs of the Faculty of Engineering, Nagoya (Japan) University, Vol. 6, No. 2.

Zalik, R.A., 1987, "The Jeffcott Equations in Nonlinear Rotordynamics," NASA/ASEE Faculty Fellowship Report, NASA Marshall, Huntsville, Alabama.

APPENDIX A

DISCRETIZED FORM OF TRANSITION MATRIX FORMULATION

The solution of the first order differential equations in vector form, or

$$\{\dot{u}\} = [\alpha]\{u\} + \{P\} \tag{A1}$$

can be written as

$$\{u(t)\} = e^{[\alpha]t}\{u(0)\} + {}_0\int^t e^{[\alpha](t-\tau)}\{P(t)\}\, d\tau \tag{A2}$$

The solution of Eq. (A2) is casted in discretized form as

$$\{u(t_{i+1})\} = e^{[\alpha]T}\{u(t_i)\} + \int_{t_i}^{t_{i+1}} e^{[\alpha](t_{i+1}-t)}\{P(t)\}\, dt, \tag{A3}$$

where $T = t_{i+1} - t_i$

Take the forcing function as linear within each increment T, or

$$\{P(t)\} = \{P(t_i)\} + \frac{t-t_i}{T}\left(\{P(t_{i+1})\} - \{P(t_i)\}\right) \tag{A4}$$

Let $[Q(t)] = e^{[\alpha]T}$

Substitute (A4) into (A3) to yield

$$\{u(t_{i+1})\} = [Q(T)]\{u(t_i)\} + \int_{t_i}^{t_{i+1}} e^{[\alpha](t_{i+1}-t)}$$

$$\left[\{P(t_i)\} + \frac{t-t_i}{T}\left(\{P(t_{i+1})\} - \{P(t_i)\}\right)\right] dt$$

$$= [Q(T)]\{u(t_i)\} + \left(\int_{t_i}^{t_{i+1}} e^{[\alpha](t_{i+1}-t)}dt\right)\{P(t_i)\}$$

$$+ \left(\int_{t_i}^{t_{i+1}} e^{[\alpha](t_{i+1}-t)}(t-t_i)dt\right)\frac{\{P(t_{i+1})\} - \{P(t_i)\}}{T} \qquad (A5)$$

$$[\alpha](t_{i+1}-t) = [\alpha].T - [\alpha](t-t_i),$$

Then

$$\int_{t_i}^{t_{i+1}} e^{[\alpha](t_{i+1}-t)}dt = \int_{t_i}^{t_{i+1}} e^{[\alpha]T-[\alpha](t-t_i)}dt$$

$$= \left(\int_{t_i}^{t_{i+1}} e^{[\alpha]T-[\alpha](t-t_i)}\, d[\alpha]t\right) \cdot [\alpha]^{-1}$$

$$= -\left(\int_{t_i}^{t_{i+1}} e^{[\alpha]T-[\alpha](t-t_i)}\, d\{[\alpha]T - [\alpha](t-t_i)\}\right)[\alpha]^{-1}$$

$$= -\, e^{[\alpha]T-[\alpha](t-t_i)}\Big|_{t_i}^{t_{i+1}} [\alpha]^{-1}$$

$$= -\left(e^{[\alpha]T-[\alpha](t_{i+1}-t_i)} - e^{[\alpha]T-[\alpha](t_i-t_i)}\right) \cdot [\alpha]^{-1}$$

$$= -\left(e^{[0]} - e^{[\alpha]T}\right)[\alpha]^{-1}$$

$$= \left(e^{[\alpha]T} - [I]\right)[\alpha]^{-1}$$

$$= \left(Q(T) - [I]\right)[\alpha]^{-1} \qquad (A6)$$

Similarly,

$$\int_{t_i}^{t_{i+1}} e^{[\alpha](t_{i+1}-t)}\,(t-t_i)dt = \int_{t_i}^{t_{i+1}} e^{[\alpha]T-[\alpha](t-t_i)}(t-t_i)dt$$

$$= e^{[\alpha]T}\int_{t_i}^{t_{i+1}} e^{[\alpha](t_i-t)}(t_i-t)\,d\,(t_i-t)$$

$$= e^{[\alpha]T}\left(\int_{t_i}^{t_{i+1}} e^{[\alpha](t_i-t)}[\alpha](t_i-t)\,d\,\{[\alpha](t_i-t)\}\right)[\alpha]^{-2}$$

$$= e^{[\alpha]T}(e^{-[\alpha]T}\{-[\alpha]T - [\hat{I}]\} + [\hat{I}])[\alpha]^{-2}$$

$$= -[\alpha]^{-1}T + (Q(T) - [\hat{I}])[\alpha]^{-2} \qquad \text{(A7)}$$

Substituting (A6) and (A7) into (A5) yields

$$\{u(t_{i+1})\} = [Q(T)]\{u(t_i)\} + ([Q(T)] - [\hat{I}])[\alpha]^{-1}(\{P(t_i)\} +$$

$$[\alpha]^{-1}\frac{\{P(t_{i+1})\} - \{P(t_i)\}}{T}) - [\alpha]^{-1}(\{P(t_{i+1})\} - \{P(t_i)\}) \qquad \text{(A8)}$$

APPENDIX B

DISCRETIZED FORM OF THE DUHAMEL INTEGRAL SOLUTION

Consider the uncoupled set of differential equations in terms of the generalized coordinates $\{q\}$

$$\{\ddot{q}\} + [D]\{\dot{q}\} + [\Lambda]\{q\} = \{P\} \tag{B1}$$

where

$$[D] = [C] = [2\xi\omega_n]$$

$$[\Lambda] = [\omega_n^2] \qquad \omega_n\text{: undamped natural frequency}$$

The solution of (B1) is

$$\{q(t)\} = [e^{-\xi\omega_n t}\cos\ \omega_d t]\{q(0)\} + \left[\frac{1}{\omega_d} e^{-\xi\omega_n t}\sin\ \omega_d t\right] \cdot$$

$$(\{\dot{q}(0)\} + \xi\omega_n\{q(0)\})$$

$$+ \int_0^t \left[\frac{1}{\omega_d} e^{-\xi\omega_n(t-\tau)}\sin\ \omega_d(t-\tau)\right]\{P(\tau)\}d\tau \tag{B2}$$

where ω_d = damped natural frequency.

$$\text{Let } \{h(t)\} = \int_0^t \left[\frac{1}{\omega_d} e^{-\xi\omega_n(t-\tau)}\sin\ \omega_d(t-\tau)\right]\{P(\tau)\}d\tau \tag{B3}$$

P(t) is linearlized so that

$$\{P(t)\} = \left\{P_i + \frac{\tau - t_i}{T}(P_{i+1} - P_i)\right\}$$

Substituting P(t) into (B3) and casting it in discretized form, one obtains

$$\{h(t)\} = \{h(t_i)\} + \int_{t_i}^{t_{i+1}} \left[\frac{1}{\omega_d} e^{-\xi\omega_n(t-\tau)} \sin \omega_d(t-\tau)\right] \cdot \left\{P_i + \frac{\tau-t_i}{T}(P_{i+1} - P_i)\right\} d\tau \qquad (B3)$$

or

$$\{h(t)\} = \{h(t_i)\} + \{\Delta h(t)\} \qquad (B4)$$

For the velocity,

$$\{\dot{h}(t)\} = \{\dot{h}(t_i)\} + \{\Delta \dot{h}(t)\} \qquad (B5)$$

Let h(t) and $\Delta h(t)$ stand for elements in vectors $\{h(t)\}$ and $\{\Delta h(t)\}$, respectively, and P_i for an element of $\{P_i\}$, then

$$\Delta h(t) = \frac{1}{\omega_d} \int_{t_i}^{t_{i+1}} e^{-\xi\omega_n(t-\tau)} \sin \omega_d(t-\tau) \cdot \left[P_i + \frac{\tau-t_i}{T}(P_{i+1} - P_i)\right] d\tau$$

$$= \frac{1}{\omega_d} e^{-\xi\omega_n(t-\tau)} \int_{t_i}^{t_{i+1}} e^{\xi\omega_n\tau} \sin \omega_d(t-\tau) \cdot \left[P_i + \frac{\tau-t_i}{T}(P_{i+1} - P_i)\right] d\tau \qquad (B6)$$

$$\Delta h(t) = \frac{1}{\omega_d} e^{-\xi\omega_n t} (INT1 + INT2) \qquad (B7)$$

In INT1,

$$\int_{t_i}^{t_{i+1}} e^{\xi\omega_n t} \sin \omega_d(t-\tau)\, d\tau$$

$$= \int_{t_i}^{t_{i+1}} e^{\xi\omega_n t} (\sin \omega_d t \cos \omega_d \tau - \cos \omega_d t \sin \omega_d \tau)\, d\tau \quad (B8)$$

$$= \sin bt \int_{t_i}^{t_{i+1}} e^{a\tau} \cos b\tau d\tau - \cos bt \int_{t_i}^{t_{i+1}} e^{a\tau}(\sin b\tau) d\tau \quad (B9)$$

where $a = \xi\omega_n$ and $b = \omega_d$

Then, from eq. (B6),(B7) and using equation (B 9) (B10)

$$INT1 = [P_i - \frac{t_i}{T} (P_{i+1} - P_i)] \int_{t_i}^{t_{i+1}} e^{\xi\omega_n\tau} \sin \omega_d (t-\tau)\, d\tau$$

$$= [P_i - \frac{t_i}{T} (P_{i+1} - P_i)] \{\frac{\sin bt}{a^2+b^2} [e^{at_{i+1}} (a \cos bt_{i+1} + b \sin bt_{i+1})$$

$$- e^{at_i}(a \cos bt_i + b \sin bt_i)]$$

$$- \frac{\cos bt}{a^2+b^2} [e^{at_{i+1}} (a \sin bt_{i+1} + b \cos bt_{i+1})$$

$$- e^{at_i}(a \sin bt_i - b \cos bt_i)]\} \quad (B11)$$

In INT2,

$$\int_{t_i}^{t_{i+1}} \tau e^{\xi\omega_n\tau} \sin \omega_d (t-\tau)\, d\tau$$

$$= \int_{t_i}^{t_{i+1}} \tau e^{\xi\omega_n\tau} (\sin \omega_d t \cos \omega_d \tau - \cos \omega_d t \sin \omega_d \tau)\, d\tau$$

$$= \sin bt \int_{t_i}^{t_{i+1}} \tau e^{a\tau} \cos b\tau \, d\tau - \cos bt \int_{t_i}^{t_{i+1}} \tau e^{a\tau} \sin b\tau d\tau \quad \text{(B12)}$$

$$= \frac{\sin bt}{a^2+b^2} \{\tau e^{a\tau}(a \cos b\tau + b \sin b\tau) - \frac{e^{a\tau}}{a^2+b^2} \cdot$$

$$(a^2 \cos b\tau + 2ab \sin b\tau - b^2 \cos b\tau)\} \Big|_{t_i}^{t_{i+1}}$$

$$- \frac{\cos bt}{a^2+b^2} \{\tau e^{a\tau}(a \sin b\tau - b \cos b\tau) - \frac{e^{a\tau}}{a^2+b^2} \cdot$$

$$(a^2 \sin b\tau - 2ab \cos b\tau - b^2 \cos b\tau)\} \Big|_{t_i}^{t_{i+1}}$$

From eq. (B6),(B7) and rearranging

$$\text{INT2} = \frac{P_{i+1}-P_i}{T} \int_{t_i}^{t_{i+1}} \tau e^{\xi\omega_n\tau} \sin \omega_d(t-\tau) d\tau$$

$$= \frac{P_{i+1}-P_i}{T} \{\frac{\sin bt}{a^2+b^2} [t_{i+1} e^{at_{i+1}}(a \cos bt_{i+1} + b \sin bt_{i+1})$$

$$- \frac{e^{at_{i+1}}}{a^2+b^2} (a^2 \cos bt_{i+1} + 2ab \sin bt_{i+1} - b^2 \cos bt_{i+1})$$

$$- t_i e^{at_i} (a \cos bt_i + b \sin bt_i) + \frac{e^{at_i}}{a^2+b^2} \cdot$$

$$(a^2 \cos bt_i + 2ab \sin bt_i - b^2 \cos bt_i)] - \frac{\cos bt}{a^2+b^2}$$

$$[t_{i+1} e^{at_{i+1}} (a \sin bt_{i+1} - b \cos bt_{i+1})$$

$$- \frac{e^{at_{i+1}}}{a^2+b^2} (a^2 \sin bt_{i+1} - 2ab \cos bt_{i+1} - b^2 \sin bt_{i+1})$$

$$- t_i e^{at_i} (a \sin bt_i - b \cos bt_i) + \frac{e^{at_i}}{a^2+b^2} \cdot$$

$$(a^2 \sin bt_i - 2ab \cos bt_i - b^2 \sin bt_i)]\} \qquad (B13)$$

The sum INT1 + INT2 is calculated from equations (B11) and (B13). Let

$$INT1 + INT2 = \frac{\sin bt}{(a^2+b^2)} \cdot SUMS - \frac{\cos bt}{(a^2+b^2)} \cdot SUMC \qquad (B14)$$

where

$$SUMS = [P_i - \frac{t_i}{T} (P_{i+1} - P_i)][e^{at_{i+1}} (a \cos bt_{i+1} + b \sin bt_{i+1})$$

$$- e^{at_i} (a \cos bt_i + b \sin bt_i)] + \frac{(P_{i+1}-P_i)}{T} \cdot$$

$$[t_{i+1} e^{at_{i+1}} (a \cos bt_{i+1} + b \sin bt_{i+1})$$

$$- \frac{e^{at_{i+1}}}{a^2+b^2} (a^2 \cos bt_{i+1} + 2ab \sin bt_{i+1} - b^2 \cos bt_{i+1})$$

$$- t_i e^{at_i} (a \cos bt_i + b \sin bt_i) + \frac{e^{at_i}}{a^2+b^2} \cdot$$

$$(a^2 \cos bt_i + 2ab \sin bt_i - b^2 \cos bt_i)]$$

$$= e^{at_{i+1}} (a \cos bt_{i+1} + b \sin bt_{i+1}) \cdot$$

$$\overbrace{[P_i - \frac{t_i}{T}(P_{i+1} - P_i) + \frac{t_{i+1}}{T}(P_{i+1} - P_i)]}^{P_{i+1}}$$

$$+ \frac{P_{i+1}-P_i}{T} \quad \frac{1}{a^2+b^2}(a^2 \cos bt_{i+1} + 2ab \sin bt_{i+1}$$

$$- b^2 \cos bt_{i+1})(-e^{at_{i+1}})$$

$$- P_i e^{at_i}(a \cos bt_i + b \sin bt_i) + \frac{P_{i+1}-P_i}{T} \quad \frac{1}{a^2+b^2} \cdot$$

$$(a^2 \cos bt_i + 2ab \sin bt_i - b^2 \cos bt_i) e^{at_i} \qquad (B15)$$

$$SUMC = [P_i - \frac{t_i}{T}(P_{i+1} - P_i)][e^{at_{i+1}}(a \sin bt_{i+1} - b \cos bt_{i+1})$$

$$- e^{at_i}(a \sin bt_i - b \cos bt_i)] + \frac{(P_{i+1}-P_i)}{T} \cdot$$

$$[t_{i+1} e^{at_{i+1}}(a \sin bt_{i+1} - b \cos bt_{i+1})$$

$$- \frac{e^{at_{i+1}}}{a^2+b^2}(a^2 \sin bt_{i+1} - 2ab \cos bt_{i+1} - b^2 \sin bt_{i+1})$$

$$- t_i e^{at_i}(a \sin bt_i - b \cos bt_i) + \frac{e^{at_i}}{a^2+b^2} \cdot$$

$$(a^2 \sin bt_i - 2ab \cos bt_i - b^2 \sin bt_i)]$$

$$= e^{at_{i+1}}(a \sin bt_{i+1} - b \cos bt_{i+1}) \cdot$$

$$\overbrace{\left[P_i - \frac{t_i\,(P_{i+1}-P_i)}{T} + \frac{t_{i+1}\,(P_{i+1}-P_i)}{T}\right]}^{P_{i+1}}$$

$$+ \frac{P_{i+1}-P_i}{T} \quad \frac{1}{a^2+b^2}\,(a^2 \sin bt_{i+1} - 2ab \cos bt_{i+1}$$

$$- b^2 \sin bt_{i+1})(-e^{at_{i+1}})$$

$$- P_i\, e^{at_i}\,(a \sin bt_i - b \cos bt_i) + \frac{P_{i+1}-P_i}{T} \quad \frac{1}{a^2+b^2} \cdot$$

$$(a^2 \sin bt_i - 2ab \cos bt_i - b^2 \sin bt_i)\, e^{at_i} \qquad \text{(B16)}$$

Substitute INT1 and INT2 in eq. (B15) and (B16) into eq. (B7) and recall that $a = \xi_n\omega_n$ and $b = \omega_d$, one arrives at

$$\Delta h(t) = \frac{e^{-at}\, e^{at_{i+1}} \sin bt}{b(a^2+b^2)}\, A_{i+1} - \frac{e^{-at}\, e^{at_{i+1}} \cos bt}{b(a^2+b^2)}\, B_{i+1} \qquad \text{(B17)}$$

where

$$A_{i+1} = P_{i+1}\,(a \cos bt_{i+1} + b \sin bt_{i+1})$$

$$- \frac{P_{i+1} - P_i}{T(a^2+b^2)}\,(a^2 \cos bt_{i+1} + 2ab \sin bt_{i+1} - b^2 \cos bt_{i+1})$$

$$+ \frac{P_{i+1} - P_i}{T(a^2+b^2)}\, e^{-aT}\,(a^2 \cos bt_i + 2ab \sin bt_i - b^2 \cos bt_i)$$

$$- P_i\, e^{-aT}\,(a \cos bt_i + b \sin bt_i) \qquad \text{(B18)}$$

$$B_{i+1} = P_{i+1} (a \sin bt_{i+1} - b \cos bt_{i+1})$$

$$- \frac{P_{i+1} - P_i}{T(a^2+b^2)} (a^2 \sin bt_{i+1} - 2ab \cos bt_{i+1} - b^2 \sin bt_{i+1})$$

$$+ \frac{P_{i+1} - P_i}{T(a^2+b^2)} e^{-aT} (a^2 \sin bt_i - 2ab \cos bt_i - b^2 \sin bt_i)$$

$$- P_i e^{-aT} (a \sin bt_i - b \cos bt_i) \qquad (B19)$$

Take derivative of (B17),

$$\dot{\Delta h}(t) = \frac{e^{at_{i+1}}}{b(a^2+b^2)} (- ae^{-at} \sin bt + b e^{-at} \cos bt) A_{i+1}$$

$$+ \frac{e^{at_{i+1}}}{b(a^2+b^2)} (ae^{-at} \cos bt + b e^{-at} \sin bt) B_{i+1} \qquad (B20)$$

For t = NT, from (B3), N is an arbitrary integer,

$$h(t)_{t=NT} = \int_0^t [\frac{1}{\omega_d} e^{-\xi\omega_n(t-\tau)} \sin \omega_d (t-\tau) P(\tau)] d\tau$$

$$= \int_0^t [\cdot] d\tau$$

$$= \int_0^T [\cdot] d\tau + \int_T^{2T} [\cdot] d\tau + \ldots + \int_{(N-1)T}^{NT} [\cdot] d\tau \qquad (B21)$$

Let $fs(t) = \frac{e^{-at} \sin bt}{b(a^2+b^2)}$, $fc(t) = \frac{e^{-at} \cos bt}{b(a^2+b^2)}$ (B22)

Substitute eq. (B17), (B22) into (B21) yields

$$h(t)_{t=NT} = fs(t)\, e^{aT} A_1 - fc(t)\, e^{aT} B_1$$

$$+ fs(t)\, e^{a(2T)} A_2 - fc(t)\, e^{a(2T)} B_2$$

$$+ \ldots\ldots fs(t) e^{aNT} A_N - fc(t)\, e^{aNT} B_N$$

$$= fs(t)\, [e^{aT} A_1 + e^{a2T} A_2 + \ldots e^{aNT} A_N]$$

$$+ fc(t)\, [e^{aT} B_1 + e^{a2T} B_2 + \ldots + e^{aNT} B_N] \qquad \text{(B23)}$$

Since $e^{-at} = e^{-aNT}$ in (B22) for $t = NT$, then eq. (B23) becomes

$$h(t)_{t=NT} = \frac{\sin bt}{b(a^2+b^2)} [e^{-a(N-1)T} A_1 + e^{-a(N-2)T} A_2 + \ldots + A_N]$$

$$+ \frac{\cos bt}{b(a^2+b^2)} [e^{-a(N-1)T} B_1 + e^{-a(N-2)T} B_2 + \ldots + B_N] \qquad \text{(B24)}$$

$$= \frac{\sin bt}{b(a^2+b^2)} \cdot [EA_N] + \frac{\cos bt}{b(a^2+b^2)} \cdot [EB_N] \qquad \text{(B25)}$$

Now, consider $t = (N+1)T$, equation (B21) is written as

$$h(t)_{t=(N+1)T} = \int_0^T [\cdot]\, d\tau + \int^{2T} [\cdot]\, d\tau + \ldots. +$$

$$\int_{(N-1)T}^{NT} [\cdot]\, d\tau + \int_{NT}^{(N+1)T} [\cdot]\, d\tau \qquad \text{(B26)}$$

Equation (B23) is then written as

$$h(t)_{t=(N+1)T} = fs(t)\ [e^{aT} A_1 + ... + e^{aNT} A_N + e^{a(N+1)T} A_{N+1}]$$

$$+ fc(t)\ [e^{aT} B_1 + ... + e^{aNT} B_N + e^{a(N+1)T} B_{N+1}] \quad (B27)$$

Since $e^{-at} = e^{-a(N+1)T}$, eq. (B26) takes the form

$$h(t)_{t=(N+1)T} = \frac{\sin bt}{b(a^2+b^2)}\ [e^{-aNT} A_1 + e^{-a(N-1)T} A_2 + ... + A_{N+1}]$$

$$+ \frac{\cos bt}{b(a^2+b^2)}\ [e^{-aNT} B_1 + e^{-a(N-1)T} B_2 + ... + B_{N+1}]$$

$$= \frac{\sin bt}{b(a^2+b^2)}\ [e^{-aT}\ (e^{-a(N-1)T} A_1 + e^{-a(N-2)T} A_2 + ... A_N) + A_{N+1}]$$

$$+ \frac{\cos bt}{b(a^2+b^2)}\ [e^{-aT}\ (e^{-a(N-1)T} B_1 + e^{-a(N-2)T} B_2 + ... B_N) + B_{N+1}]$$

$$= \frac{\sin bt}{b(a^2+b^2)}\ [e^{-aT} \cdot EA_N + A_{N+1}]$$

$$+ \frac{\cos bt}{b(a^2+b^2)}\ [e^{-aT} \cdot EB_N + EB_{N+1}] \quad (B28)$$

From (B25) and B28) the following equation for t=(N+2)T can be written as

$$h(t)_{t=(N+2)T} = \frac{\sin bt}{b(a^2+b^2)}\ [e^{-aT} \cdot EA_{N+1} + A_{N+2}]$$

$$+ \frac{\cos bt}{b(a^2+b^2)} [e^{-aT} \cdot EB_{N+1} + B_{N+2}] \qquad (B29)$$

where

$$EA_{N+1} = e^{-aT} \cdot EA_N + A_{N+1}$$

$$EB_{N+1} = e^{-aT} \cdot EB_N + B_{N+1} \qquad (B30)$$

and EA_N, EB_N are defined in eq. (B24) and (B25), they are:

$$EA_N = e^{-a(N-1)T} A_1 + e^{-a(N-2)T} A_2 + ... A_N$$

$$EB_N = e^{-a(N-1)T} B_1 + e^{-a(N-2)T} B_2 + ... B_N \qquad (B31)$$

And A_N, B_N are defined in eq. (B18), (B19).

Finally, one arrives at

$$h(t) = \frac{\sin bt}{b(a^2+b^2)} \cdot EA_N + \frac{\cos bt}{b(a^2+b^2)} \cdot EB_N$$

; t = NT, T is the time step (B32)

where EA_N, EB_N are defined in (B31) and can be calculated directly from previous EA_{N-1} and EB_{N-1} of time t = (N-1)T, that is,

$$EA_N = e^{-aT} \cdot EA_{N-1} + A_N$$

$$EB_N = e^{-aT} \cdot EB_{N-1} + B_N \qquad (B33)$$

The same procedure can be followed to obtain $\dot{h}(t)$ starting from eq. (B20) with the result

$$\dot{h}(t) = \frac{-a \sin bt + b \cos bt}{b(a^2+b^2)} \cdot EA_N + \frac{a \cos bt + b \sin bt}{b(a^2+b^2)} \cdot EB_N$$

; t = NT, T is time step (B34)

Eq. (B32) is written in vector form and is substituted into (B2) to yield

$$\{q(t)\} = [e^{-\xi\omega_n t} \cos \omega_d t] \{q(0)\} + [\frac{1}{\omega_d} e^{-\xi\omega_n t} \sin \omega_d t] \cdot$$

$$(\{\dot{q}(0)\} + \xi\omega_n \{q(0)\})$$

$$+ \{\frac{\sin bt}{b(a^2+b^2)} \cdot EA_N + \frac{\cos bt}{b(a^2+b^2)} \cdot EB_N\}, \quad t = NT \qquad (B35)$$

For $\{\dot{q}\}$, derivative of (B2) for the first two terms at the right hand side is taken and then substitution is made of eq. (B34) into the resulting relationship to yield

$$\{\dot{q}(t)\} = [-e^{-\xi\omega_n t} (\xi\omega_n \cos \omega_d t + \omega_d \sin \omega_d t] \{q(0)\}$$

$$+ [e^{-\xi\omega_n t} (-\frac{1}{\omega_d} \xi\omega_n \sin \omega_d t + \cos \omega_d t)] \cdot$$

$$(\{\dot{q}(0)\} + \xi\omega_n \{q(0)\})$$

$$+ \{\frac{-a \sin bt + b \cos bt}{b(a^2+b^2)} \cdot EA_N + \frac{a \cos bt + b \sin bt}{b(a^2+b^2)} \cdot EB_N\}$$

; t = NT (B36)

Equations (B35) and (B36) are written in discretized form, and recalling that $a = \xi_n \omega_n$, $b = \omega_d$, $t = t_{i+1} = (N+1)T$, one can write

$$\{q(t_{i+1})\} = [e^{-at_{i+1}} \cos bt_{i+1}]\{q(0)\}$$

$$+ [\frac{1}{b} e^{-at_{i+1}} \sin bt_{i+1}](\{\dot{q}(0)\} + a\{q(0)\})$$

$$+ \{\frac{\sin bt_{i+1}}{b(a^2+b^2)} \cdot EA_{N+1} + \frac{\cos bt_{i+1}}{b(a^2+b^2)} \cdot EB_{N+1}\} \qquad (B37)$$

$$\{\dot{q}(t_{i+1})\} = [-e^{-at_{i+1}} (a \cos bt_{i+1} + b \sin bt_{i+1}]\{q(0)\}$$

$$+ [e^{-at_{i+1}} (-\frac{1}{b} a \sin bt_{i+1} + \cos bt_{i+1})](\{\dot{q}(0)\} + a\{q(0)\})$$

$$+ \{\frac{-a \sin bt_{i+1} + b \cos bt_{i+1}}{b(a^2+b^2)} \cdot EA_{N+1}$$

$$+ \frac{a \cos bt_{i+1} + b \sin bt_{i+1}}{b(a^2+b^2)} \cdot EB_{N+1}\} \qquad (B38)$$

where

EA, EB are defined in (B30),(B31) and A, B in (B30),(B31) are defined in (B18), (B19).

APPENDIX C

FOURTH ORDER RUNGE-KUTTA WITH ITERATION

The equations ofmotion for both housing and motor can be cast in the first order form

$$\dot{y} = f(t,y) \qquad (C1)$$

For the coefficients K_2 and K_3 of the 4th order Runge-Kutta Method, the coupling forces in the right hand side of equation (C1) are assumed to be linear within each time increment $T = t_{i+1} - t_i$. The physical coupling forces, $\{F_I\}$ at time $t_i + T/2$ are assumed then as

$$\{F_I(t_i + \frac{T}{2})\} = \frac{1}{2}\left(F_I(t_i) + F_I(t_{i+1})\right)$$